AECL EACL

CA9700637

AECL-11494-3, COG-95-552-3

The Disposal of Canada's Nuclear Fuel Waste: A Study of Postclosure Safety of In-Room Emplacement of Used CANDU Fuel in Copper Containers in Permeable Plutonic Rock Volume 3: Geosphere Model

Le stockage permanent des déchets de combustible nucléaire du Canada : Étude de la sûreté post-fermeture de la mise en place en chambre du combustible CANDU irradié renfermé dans des conteneurs en cuivre enfouis dans la roche plutonique perméable Volume 3 : Modèle de géosphère

F.W. Stanchell, C.C. Davison, T.W. Melnyk, N.W. Scheier, T. Chan

June 1996 juin

THE DISPOSAL OF CANADA'S NUCLEAR FUEL WASTE: A STUDY OF POSTCLOSURE SAFETY OF IN-ROOM EMPLACEMENT OF USED CANDU FUEL IN COPPER CONTAINERS IN PERMEABLE PLUTONIC ROCK VOLUME 3: GEOSPHERE MODEL

by

F.W. Stanchell, C.C. Davison, T.W. Melnyk, N.W. Scheier and T. Chan

Atomic Energy of Canada Limited
Whiteshell Laboratories
Pinawa, Manitoba R0E 1L0
1996

AECL-11494-3
COG-95-552-3

THE DISPOSAL OF CANADA'S NUCLEAR FUEL WASTE: A STUDY OF POSTCLOSURE SAFETY OF IN-ROOM EMPLACEMENT OF USED CANDU FUEL IN COPPER CONTAINERS IN PERMEABLE PLUTONIC ROCK VOLUME 3: GEOSPHERE MODEL

by

F.W. Stanchell, C.C. Davison, T.W. Melnyk, N.W. Scheier and T. Chan

ABSTRACT

This report discusses the approach we used to develop a model of the 3-D network of transport pathways through the geosphere from the location of a nuclear fuel waste disposal vault at a depth of 500 m in a hypothetical permeable plutonic rock mass. The transport pathways correspond to the pathways of advective groundwater movement through this permeable rock from the disposal vault to discharge areas at groundsurface. In this analysis we assumed the permeability of the region of rock immediately surrounding the waste emplacement areas of the disposal vault was considerably higher than the permeability used in the geosphere model for the EIS case study (i.e. 10^{-17} m^2 in this study, 10^{-19} m^2 in the EIS case study). We also assumed the porosity of the rock could fall within the range 10^{-3} to 10^{-5} to represent the range of effects by alternative conceptual models of flow through fracture networks in the rock. Molecular diffusion is not a significant transport mechanism in this geosphere model whereas molecular diffusion was the dominant transport mechanism through the rock in the near field of the vault in the geosphere model of the EIS case study. Advection by the groundwater flow field in the rock surrounding the disposal vault entirely controls the rate and direction of transport from the vault in this geosphere model.

The hydrogeological environment we assumed for this geosphere model is entirely hypothetical, unlike the model we developed for the EIS case study which was a conservative, yet realistic, representation of the hydrogeological conditions encountered at the site of our Underground Research Laboratory in the Whiteshell Research Area. We used the same geometry of rock structures for this model as we used in the geosphere model for the EIS case study but we assigned hydrogeologic properties to the various rock domains of the model that result in relatively rapid groundwater flow from the depth of the disposal vault to surface discharge areas. We have not encountered such hydrogeological conditions at the Whiteshell Research Area nor below depths of 500 m at any of our other geologic research areas on the Canadian Shield. However, Swedish and Finnish assessments of repositories for nuclear fuel waste disposal have assumed similar hydrogeologic conditions for rocks of the Fennoscandian Shield to depths of 600 m.

This report describes the modelling and sensitivity analyses we performed with the MOTIF finite element model to develop the GEONET transport network for this hypothetical geosphere situation. The geosphere model accounts for the effects of natural geothermal heat and vault-induced heat on transport pathways. The model also incorporates the effects of a groundwater supply well drawing water from a fracture zone in the rock mass.

Atomic Energy of Canada Limited
Whiteshell Laboratories
Pinawa, Manitoba R0E 1L0
1996

AECL-11494-3
COG-95-552-3

LE STOCKAGE PERMANENT DES DÉCHETS DE COMBUSTIBLE NUCLÉAIRE DU CANADA : ÉTUDE DE LA SÛRETÉ POST-FERMETURE DE LA MISE EN PLACE EN CHAMBRE DU COMBUSTIBLE CANDU IRRADIÉ RENFERMÉ DANS DES CONTENEURS EN CUIVRE ENFOUIS DANS LA ROCHE PLUTONIQUE PERMÉABLE VOLUME 3 : MODÈLE DE GÉOSPHÈRE

par

F.W. Stanchell, C.C. Davison, T.W. Melnyk, N.W. Scheier et T. Chan

RÉSUMÉ

Dans le présent rapport, nous examinons la méthode employée en vue d'élaborer un modèle du réseau tridimensionnel des voies de transport dans la géosphère ayant comme origine une installation de stockage permanent des déchets de combustible nucléaire à une profondeur de 500 m dans un massif hypothétique de roche plutonique perméable. Les voies de transport correspondent aux trajectoires de circulation par advection des eaux souterraines dans la roche perméable à partir de l'installation de stockage permanent jusqu'aux aires de décharge à la surface du sol. Dans cette analyse, nous avons supposé que la perméabilité de la région rocheuse à la périphérie immédiate des zones de mise en place des déchets de l'installation de stockage était considérablement plus élevée que celle utilisée dans le modèle de géosphère servant à l'étude de cas de l'EIE (c.-à-d. 10^{-17} m^2 dans la présente étude et 10^{-19} m^2 dans l'étude de cas de l'EIE). Nous avons également supposé que la porosité de la roche pourrait s'établir entre 10^{-3} et 10^{-5} afin de représenter toute la gamme des effets par d'autres modèles conceptuels d'écoulement dans des réseaux de fractures dans le massif rocheux. La diffusion moléculaire ne constitue pas un mécanisme de transport important dans ce modèle de géosphère, tandis que la diffusion moléculaire représentait le mécanisme de transport principal dans la roche du champ proche de l'installation de stockage dans le modèle de géosphère de l'étude de cas de l'EIE. L'advection due au champ d'écoulement des eaux souterraines dans le massif rocheux à la périphérie de l'installation de stockage régit entièrement la vitesse et la direction du transport en provenance de l'installation dans ce modèle de géosphère.

Le milieu hydrogéologique pris pour ce modèle de géosphère est entièrement hypothétique, au contraire du modèle que nous avons élaboré pour l'étude de cas de l'EIE qui représentait de façon prudente quoique réaliste les conditions hydrogéologiques que l'on rencontre au site de notre Laboratoire de recherches souterrain dans l'Aire de recherches de Whiteshell. Dans ce modèle, nous nous sommes servis de la même géométrie des structures rocheuses que dans le modèle de géosphère de l'étude de cas de l'EIE, mais nous avons affecté aux divers domaines rocheux du modèle des propriétés hydrogéologiques qui se traduisent par des temps de parcours relativement courts des eaux souterraines de la profondeur de l'installation de stockage jusqu'aux aires de décharge à la surface. Nous n'avons rencontré de telles conditions

hydrogéologiques ni dans l'Aire de recherches de Whiteshell ni à des profondeurs au-dessous de 500 m dans toutes nos autres aires de recherches géologiques dans le Bouclier canadien. Toutefois, dans des études suédoises et finlandaises réalisées en vue d'évaluer des dépôts destinés au stockage permanent de déchets de combustible nucléaire, on a supposé des conditions hydrogéologiques similaires correspondant à des massifs rocheux du Bouclier fennoscandien à des profondeurs de 600 m.

Le présent rapport décrit la modélisation et les analyses de sensibilité que nous avons réalisées à l'aide du modèle à éléments finis MOTIF en vue d'élaborer le réseau de transport GEONET pour cette situation de géosphère hypothétique. Ce modèle de géosphère tient compte des effets de la chaleur géothermique naturelle et de la charge thermique de l'installation de stockage sur les voies de transport. Le modèle englobe également les effets d'un puits d'alimentation en eau souterraine qui soutire de l'eau issue d'une zone de fracture dans le massif rocheux.

Énergie atomique du Canada limitée
Laboratoires de Whiteshell
Pinawa (Manitoba) R0E 1L0
1996

AECL-11494-3
COG-95-552-3

CONTENTS

LIST OF TABLES

LIST OF FIGURES

continued...

LIST OF FIGURES (concluded)

PREFACE

The concept for disposal of Canada's nuclear fuel waste involves isolating the waste in corrosion-resistant containers emplaced and sealed within a vault at a depth of 500 to 1000 m in plutonic rock of the Canadian Shield. The technical feasibility and social aspects of the concept, and its impact on the environment and human health, are presented in an Environmental Impact Statement (EIS) (AECL 1994a), a summary of the EIS (AECL 1994b) and a set of nine primary references (Davis et al. 1993; Davison et al. 1994a,b; Goodwin et al. 1994; Greber et al. 1994; Grondin et al. 1994; Johnson et al. 1994a,b; Simmons and Baumgartner 1994).

The disposal concept permits a choice of methods, materials, site locations and designs (AECL 1994a,b; Johnson et al. 1994a; Simmons and Baumgartner 1994). This preface puts into perspective the following three studies which illustrate the long-term safety of different implementations of the concept:

- the postclosure assessment case study of a reference disposal system presented in the EIS (AECL 1994a,b; Goodwin et al. 1994);

- a study to illustrate how to identify a favourable vault location that would ensure long groundwater travel times from the vault to the accessible environment (Stevenson et al. 1995, 1996; Ophori et al. 1995, 1996); and

- the present study that illustrates (i) the flexibility for designing engineered barriers to accommodate a permeable host-rock condition in which advection is the rate-determining contaminant transport process (Baumgartner et al. 1996), and (ii) the flexibility of the modelling methodology to simulate the long-term performance of different design options and site characteristics (Goodwin et al. 1996, Johnson et al. 1996, Stanchell et al. 1996, Wikjord et al. 1996, Zach et al. 1996).

THE POSTCLOSURE ASSESSMENT CASE STUDY PRESENTED IN THE EIS

The EIS (AECL 1994a,b) and four of the primary references (Davis et al. 1993, Davison et al. 1994b, Goodwin et al. 1994 and Johnson et al. 1994b) describe a case study of the long-term (i.e., postclosure) performance of a hypothetical implementation of the concept, referred to as the *reference disposal system.*

The reference system illustrates what a disposal system, including the vault, geosphere and biosphere, might be like. Although it is hypothetical, it is based on information derived from extensive laboratory, field and engineering investigations. Many of the assumptions made about the long-term performance of the reference system are conservative; that is, they would tend to overestimate adverse effects. The technology specified is either available or judged to be readily achievable. The reference disposal system includes one possible choice among the options for such things as the waste form, the disposal container, the buffer and backfill, the shaft seals and bulkheads, the location and depth of the vault, and the orientation and layout of the vault with respect to the geological features of the site. The components and designs chosen for the engineered barriers and the site conditions represented in the reference system are not being recommended, but rather, they illustrate a technically feasible way of implementing the disposal concept. In an actual implementation of the concept, the engineered system would be adapted to the lithostructural, hydrogeological, geochemical, geothermal, geomechanical, and geomicrobiological conditions of the host rock formation, and the expected evolution of those conditions over thousands of years.

The *reference vault* (Johnson et al. 1994b) of the EIS postclosure assessment case study includes used-fuel bundles from CANDU® reactors, encapsulated in thin-walled Grade-2 titanium alloy containers packed with particulate for mechanical support, emplaced in boreholes in the floor of rooms, and surrounded by a sand-bentonite mixture. The rooms are filled with a lower backfill of crushed granite and lake clay and an upper backfill of sand and bentonite, and the entrances are sealed with concrete bulkheads. The plan area and the design capacity of the vault were initially set at 4.0 km^2 and 10.1 million fuel bundles (191 000 Mg U) respectively. The fuel inventory is roughly equivalent to the waste that would accrue in 100 a at the current production rates in Canada. The plan area was subsequently reduced to 3.2 km^2 and the inventory to 8.5 million bundles (162 000 Mg U), as a result of design constraints to ensure a large margin of safety in the case study. The borehole-emplacement geometry was modelled as layered planar elements (slabs) representing the waste form, buffer, backfill and host rock.

The *reference geosphere* (Davison et al. 1994b) consists of the host rock formation, its groundwater flow system, the materials used to seal the shafts and exploration boreholes, and a water well. The geological characteristics of the reference geosphere are derived from data from AECL's Whiteshell Research Area (WRA), located near Lac du Bonnet, Manitoba. This area includes a substantive portion of the Lac du Bonnet Batholith, a large granitic rock body several kilometres deep with an exposed surface measuring over 60 km long and 20 km across at its widest part. The granitic body was intruded over 2.5 billion years ago into the rocks existing at the time. The batholith, the surrounding rocks, and the interfaces between them have been the subject of field investigations for more than 15 a. Most of the information about the rock mass, such as the location and orientation of fractures and fracture zones, is based on field studies of the WRA, including detailed investigations that were conducted to locate and construct an Underground Research Laboratory (URL) to a depth of 440 m. For geological structures outside the areas where detailed borehole information was available, inferences have been made on the basis of nearby boreholes; geological mapping; and satellite, airborne and ground-based geophysical surveys. The hypothetical vault for the reference system was located at a depth of 500 m within the rock mass investigated at the URL to ensure that the maximum amount of available subsurface data was used to construct the geosphere model.

In the postclosure assessment of the reference system, we assumed that a large, low-dipping, fracture zone — designated LD1 — was located close to the vault horizon. Although field evidence from the URL revealed that this fracture zone did not extend beyond a depth of about 400 m, we conservatively assumed that it continued to much greater depths and connected with other vertical fracture zones. In this situation, LD1 became a pathway for rapid groundwater flow from the depth of the hypothetical vault to the accessible environment. We constrained all waste disposal rooms to be located beneath LD1 (i.e., to the footwall side of the fracture) and imposed a waste exclusion distance of 50 m within the low-permeability, sparsely fractured rock domain between this fracture zone and the nearest waste disposal room of the vault. To accommodate the waste exclusion distance, we chose to restrict the waste capacity of the vault relative to the capacity specified in a conceptual engineering study (Simmons and Baumgartner 1994). These design constraints, together with the hydrogeological properties of the rock beneath LD1, ensured that (i) contaminants passed through the backfill, a large reservoir which reacts strongly with most of the contaminants, and (ii) diffusion was the dominant transport process from the waste disposal rooms areas through the lower rock domain to the fracture zone.

The *reference biosphere* (Davis et al. 1993) consists of the surface and near-surface environment, including the water, soil, air, people, and other organisms, as encountered on the Canadian Shield as a whole. However, the parts of the biosphere that interface with the geosphere are specific to the WRA. In all other respects, the biosphere is assumed to be typical of the Canadian Shield, consisting of rocky outcrops; bottom lands with pockets of soil, bogs, and lakes; and uplands with meadows, bush, and forests. No major changes in the topography of the region are likely to occur during the 10 000 a following closure of a disposal facility. Changes in climate, surface water flow patterns, soils, and vegetation types are expected to be within the

range of variation currently observed across the Shield; such variations are included in the distributions of values of model parameters specified for the EIS case study.

The long-term safety analyses of this system of engineered and geological barriers indicated that the maximum estimated mean dose rate to an individual in the critical group during the first 10 000 a is about 100 million times smaller than dose rate from natural background radiation. The corresponding risk is about a million times smaller than the radiological risk criterion specified by the Atomic Energy Control Board in Regulatory Document R-104 (AECB 1987).

A STUDY TO IDENTIFY A FAVOURABLE VAULT LOCATION

In an actual implementation, it would be advantageous to locate the disposal vault in a hydraulically favourable setting within the large-scale groundwater flow system of a siting area. Recently, we completed a separate study to illustrate how such a location could be found within the WRA. The conceptual hydrogeological model of the WRA was revised using information from a program of regional geologic mapping, geophysical surveys and borehole drilling and testing (Stevenson et al. 1995, 1996). Large-scale groundwater flow modelling was then performed using a three-dimensional, finite-element hydrogeological code; and groundwater travel times, flow pathways and discharge locations were determined with a particle tracking code (Ophori et al. 1995, 1996).

This study has indicated that diffusion is the rate-determining transport process and diffusive transport times greater than 10^5 a could likely be achieved by selecting a vault location at 750 m depth about 5 km northeast of the URL. Advective travel times are about two orders of magnitude longer than the diffusive transport time. Since the groundwater flow and particle-tracking analyses indicated that such a favourable location would likely ensure a margin of safety even greater than that calculated for the EIS case study, a full systems analysis was not carried out. Instead, we directed our efforts to the present study in which we evaluate the long-term effects of a hypothetical geological setting with a permeable host-rock condition.

THE PRESENT STUDY

A wide range of design options is possible within the general definition of the disposal concept (AECL 1994a,b; Johnson et al. 1994a; Simmons and Baumgartner 1994). In the present study, we illustrate the potential of designing the engineered barriers and the vault to increase the robustness of the long-term safety case, or to compensate for hydrogeological conditions that could result in a less effective geosphere barrier than the one we specified for the EIS case study. In addition, we illustrate the flexibility of the modelling approach to integrate new features, processes and data representing different design options and site characteristics into a full systems assessment. To achieve these ends, we have undertaken an analysis of the feasibility and safety of emplacing long-lasting copper containers within vault rooms (as opposed to deposition in boreholes in the floor of rooms) in a hypothetical volume of permeable plutonic rock where advective travel times from the vault to the biosphere are very short relative to those in the EIS case study. Although we have not encountered such conditions at disposal-vault depths in our investigations at various research areas on the Shield, performance assessments done for the Swedish and Finnish nuclear waste disposal programs have considered these conditions in the crystalline rocks of the Fennoscandian Shield. We are not suggesting that such rock conditions might constitute favourable, desirable, or even acceptable conditions for an eventual disposal site on the Canadian Shield. Rather, the study is intended to illustrate the effectiveness of the in-room emplacement method and copper containers in inhibiting the release of contaminants from the vault.

The vault model for the present study simulates dissolution of used CANDU fuel in a geochemical environment, which evolves from an initial oxidative condition, caused by residual air and radiolysis, to an eventual steady-state anoxic condition. The model simulating the performance of copper containers is based

on pinhole manufacturing defects and indefinite lifetime (i.e., no corrosion-induced failures). The in-room emplacement geometry is modelled as a line source representing the waste form, point sources representing pinholes in the defected containers randomly located in the vault, and concentric cylinders representing the buffer, backfill and excavation disturbed zone.

The geosphere model for the present study is more speculative than the one used for the EIS case study because it does not represent conditions we have encountered at any of our geologic research areas. We assume that the vault depth, the geometry of the geosphere model, and the arrangement of major fracture zones and rock mass domains surrounding the disposal vault are identical to those of the EIS case study. However, we assume much higher permeability and lower porosity conditions in the rock domain adjacent to the vault than the conditions observed at the URL and used in the EIS case study. As a result, the lower rock domain is not a diffusion-dominated barrier and the low-dipping fracture zone, LD1, is not the dominant advection pathway to the surface. The effects of geothermal gradient, vault heat and a water supply well on the groundwater flow field have been simulated and the implications on the long-term redox conditions in the vault have been assessed. The groundwater travel times from the disposal vault to the surface are up to 10 000 times shorter in this present geosphere model than in the model used for the EIS case study.

For this study, there is no advantage to constraining the location of the disposal rooms relative to LD1 as was done in the EIS case study. Thus the waste disposal rooms are located both below and above LD1 (i.e., on both the footwall and hangingwall sides of the fracture). The 50-m waste exclusion distance is retained but is relatively insignificant because advection is the dominant transport process in the permeable lower rock domain. Thermal restrictions and shielding requirements of the in-room emplacement option result in a reduction in the density of waste containers of roughly 50% relative to the borehole emplacement option of the EIS case study.

The biosphere model for the present study includes a number of changes, notably inclusion of additional radionuclides with shorter half-lives, inhalation pathways for animals, the most recent internal dose conversion factors of the International Commission on Radiological Protection (ICRP 1991a, b), geosphere dose limits for non-human biota, and updated values of model input parameters. Moreover, the part of the model representing the biosphere/geosphere interface was improved to account more fully for terrestrial discharge of radionuclides.

COMPARISON OF THE EIS CASE STUDY AND THE PRESENT STUDY

The key features of the EIS postclosure assessment case study and the present study are summarized as follows:

		EIS CASE STUDY	PRESENT STUDY
DESIGN CONSIDERATIONS			
Emplacement option		borehole	in-room
Vault area/depth		3.2 km^2/500 m	3.4 km^2/500 m
Fuel inventory:	number of bundles	8.5 million	4.3 million
	mass of uranium	162 000 Mg	82 000 Mg
Fuel Burnup		685 GJ/kg U	720 GJ/kg U
Fuel Cooling time		10 a	10 a
Number of bundles per container		72	72
Number of waste containers		118 700	60 100
Room locations		footwall of LD1	footwall and hangingwall of LD1

	EIS CASE STUDY	PRESENT STUDY
VAULT MODEL		
Vault model geometry	layered slabs	nested cylinders
Fuel dissolution model	thermodynamic	kinetic Container shell material
Grade-2 Ti	high purity Cu	
Container corrosion mechanisms	localized crevice and delayed hydride cracking	general corrosion and pitting
Fraction of containers failed instantly	10^{-3} to 10^{-4} (complete failure)	10^{-3} to 10^{-4} (pinhole failure)
Fraction of containers failed by 10^4 a	1.0	10^{-3} to 10^{-4}
Effective buffer thickness	0.25 m	1.48 m
Effective backfill thickness	1.4 m	0.76 m
Excavation disturbed zone	evaluated outside system model	evaluated explicity within system model
GEOSPHERE MODEL		
Conceptual model of fracture zones and rock domains	URL area of WRA	URL area of WRA*
Permeability of rock domain surrounding vault	10^{-19} m^2	10^{-17} m^2
Effective transport porosity of rock domain surrounding vault	3×10^{-3}	10^{-3} to 10^{-5}
Minimum contaminant transport times from vault to biosphere	tens of thousands of years	tens of years
Rate-determining transport process	diffusion	advection
Maximum well depth	200 m	100 m
BIOSPHERE MODEL	BIOTRAC1 - typical of the Canadian Shield	BIOTRAC2 - modifications to improve the model and update the parameters
SYSTEMS ANALYSIS		
Computer Code	third generation code (SYVAC3-CC3-ML3)	prototype (PR4) of fourth generation code (SYVAC3-CC4)
Maximum estimated dose rate to a member of critical group up to 10^4 a	about 10^{-11} Sv/a	about 10^{-6} Sv/a
Time at which estimated dose rate reaches peak	$> 10^5$ a	about 10^4 a
Key radionuclides contributing to estimated dose rate up to 10^4 a	^{129}I ^{36}Cl ^{14}C	^{129}I, ^{36}Cl ^{14}C, ^{79}Se ^{90}Sr, ^{90}Y, ^{99}Tc
Principal safety feature	low permeability rock domain surrounding vault	long-lasting containers

* The conceptual model used for this present study does not represent a combination of conditions that we have encountered at any of our geologic research areas on the Shield. It has the same geometric arrangement of fracture zones and rock domains as was used in the EIS case study; however, the permeability of the rock domain surrounding the vault has been assumed to be 10^{-17} m^2. This permeability is 100 times greater than the value specified for the EIS case study, which was based on actual measurements within the lower rock zone at the URL.

The EIS case study, the study to identify a favourable vault location, and the present study illustrate the flexibility of AECL's disposal concept in taking advantage of the retention, delay, dispersion, dilution and radioactive decay of contaminants in a system of natural barriers provided by the geosphere and the hydrosphere and of engineered barriers such as the waste form, container, buffer and backfill. In an actual implementation, the engineered system would be designed for the geological conditions encountered at the host site.

HIERARCHY AND SCOPE OF DOCUMENTS FOR THE PRESENT STUDY

This study, presented in five main volumes and a number of supporting documents, is organized as follows:

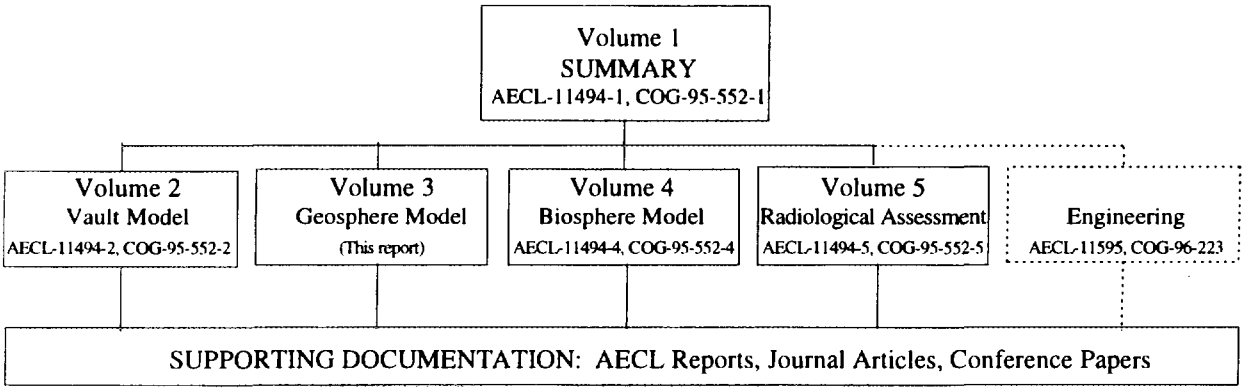

Volume 1, Summary (Wikjord et al. 1996), provides an overview of this study and summarizes the design considerations and safety of in-room emplacement of CANDU used-fuel in long-lasting copper containers in permeable plutonic rock.

Volume 2, Vault Model (Johnson et al. 1996), describes and justifies the assumptions, model and data used to analyze the long-term behaviour of the engineered system (the near-field), including the waste form (used CANDU fuel), container shell (deoxidized, low-phosphorous copper), buffer (precompacted bentonite clay and silica sand), backfill (glacial lake clay and crushed rock), and excavation disturbed zone.

Volume 3, Geosphere Model (this report), describes and justifies the assumptions, model and data used to analyze the transport of contaminants through permeable plutonic rock of the Canadian Shield, including the effects of a pumping well. The geological characteristics assumed in this study are not based on an integrated data set for any particular field research area.

Volume 4, Biosphere Model (Zach et al. 1996), describes and justifies the assumptions, model and data used to analyze the movement of contaminants through the near-surface and surface environments and to estimate radiological impacts on humans and other biota.

Volume 5, Radiological Assessment (Goodwin et al. 1996), provides an estimate of long-term radiological effects of the hypothetical disposal system on human health and the natural environment, including an analysis of how uncertainties of the assumed site and design features affect system performance.

A separate engineering study (Baumgartner et al. 1996), shown by the dotted lines, is closely linked to this 5-volume series. It describes the conceptual design, technical feasibility, thermal and mechanical analyses, and project lifecycle for implementing an engineered system based on the in-room emplacement of copper containers. It is applicable to a broader range of geosphere conditions than assumed in the present study.

1. INTRODUCTION

The geosphere model we developed for the EIS case study (Davison et al. 1994b) represented geological conditions at the Whiteshell Research Area (WRA) located near Lac du Bonnet, Manitoba. The hypothetical vault for the EIS case study was located at a depth of 500 m within the portion of the model representing the rock mass at the site of the Underground Research Laboratory (URL) where the maximum amount of subsurface data was available to construct the geosphere model. At this depth and location the rock mass at the WRA is sparsely fractured, aside from the occasional, large fracture zone and has very low permeability (10^{-19} m^2 or lower). As a result, for the EIS case study, the movement of vault contaminants through the rock immediately surrounding the waste emplacement areas of the vault was largely diffusive and the low permeability rock was very effective at inhibiting the transport of vault contaminants.

A wide range of design options is available within the general definition of the disposal concept (AECL, 1994) and the engineered barriers or vault could be designed to increase the robustness of the disposal system safety case or to compensate for a geosphere with less effective barrier characteristics than those of the EIS case study. To address this we have undertaken a study of the feasibility and safety of in-room emplacement of copper containers in a hypothetical volume of plutonic rock where advective travel times in the groundwater in the rock from the vault to the biosphere are relatively short.

The geosphere model we adopted for this study is hypothetical since it does not represent conditions we have encountered at any of our geologic research areas on the Canadian Shield. The geometry of the fracture zones and rock domains for the geosphere model in this study is identical to that used for the EIS case study. The disposal vault, representing an in-room waste emplacement design, is located at a depth of 500 m in this geosphere, at the same geometric location with respect to the rock domains and fracture zones as in the EIS case study. The rock surrounding the disposal vault is assumed to have the same arrangement of major fracture zones and rock mass domains as the previous case study. Specifically, the low dipping fracture zone, LD1, is still assumed to extend through the geosphere and some waste emplacement areas of the vault are located within 50 m of this fracture zone. As in the EIS case study we assume that a groundwater supply well could exist in the geosphere, drawing water from the low-dipping fracture zone, LD1. However, the geosphere model for this study assumes much higher permeability (10^{-17} m^2) and lower porosity conditions in the rock domain surrounding the disposal rooms than the conditions used in the EIS case study. As a result, the rock domain surrounding the disposal rooms is not a diffusion barrier to vault contaminants and the low dipping fracture zone near the disposal vault (LD1) is not the only dominant advective groundwater flow pathway to the surface as was the situation in the EIS case study. In this geosphere model, transport through the geosphere is dominated by advection in moving groundwater within the rock. The transport times along groundwater flow pathways from the disposal vault to groundsurface are 1000 to 10,000 times shorter in this geosphere model than in the model used for the EIS case study.

We are not suggesting that such rock conditions might constitute favourable, desirable or even acceptable geosphere conditions for an eventual disposal vault site on the Canadian Shield. Rather, this overall study is intended to illustrate the effectiveness of the in-room waste emplacement method of vault design (versus the borehole emplacement method of the EIS case study) and copper waste containers (versus the titanium containers of the EIS case study) in inhibiting the release of contaminants from the disposal vault. In actual practice in selecting a location for a disposal vault we would expect to be able to take

much greater advantage of the natural geosphere barrier characteristics of sites in plutonic rocks of the Canadian Shield than we have accounted for in this study. As we have discussed in Davison et al. (1994b), AECL (1994), Stevenson et al. (1995, 1996) and Ophori et al. (1995, 1996) the geosphere surrounding a disposal vault in plutonic rock of the Canadian Shield could provide a very effective barrier to the release of vault contaminants to the biosphere. This can be accomplished by: situating the waste emplacement areas of the vault in a domain of rock having very low permeability; situating the vault within a groundwater flow system where long, slow pathways from the vault to groundsurface exist; or, some combination of both of these.

In this report we document the methodology we used to develop a simplified model of the transport of vault contaminants along pathways through a hypothetical permeable geosphere surrounding a disposal vault representing the in-room emplacement of nuclear fuel wastes encapsulated in copper containers. This geosphere model (GEONET) was developed for use in an overall assessment of disposal system safety (Goodwin et al. 1996). The approach we used in developing this geosphere model is virtually the same as the approach we described in Davison et al. (1994b) for developing the geosphere model of the EIS case study. The geosphere model is derived from analysis of a detailed three-dimensional groundwater flow model of these hypothetical conditions. Groundwater flow velocities through the geosphere surrounding the disposal vault were calculated using the MOTIF finite element code (Davison et al. 1994b). Particle tracking was done using the TRACK3D code (Nakka and Chan 1995) to identify the groundwater flow paths through the geosphere from the disposal vault to discharge locations at ground surface. Five hundred and four particles were evenly distributed through the area representing the waste emplacement areas of the vault and then instantaneously released and tracked to the surface to map these pathways. The results of the particle tracking were used to determine:

1. the geometry of the contaminant transport pathways through the hypothetical permeable geosphere from the disposal vault to discharge locations in the biosphere for the GEONET model;

2. the hydraulic heads along these transport pathways under the effects of both natural geothermal gradients and thermally-driven flow from vault heating;

3. empirical equations for use in GEONET to estimate the drawdown in hydraulic heads at all nodes in transport pathways outside the fracture zone (LD1) due to pumping groundwater from a well intersecting the fracture zone to a depth of 100 m; and,

4. an empirical equation for use in GEONET which relates the size and location of the area at which these pathways emerge at surface to the well depth and pumping rate.

2. THE DETAILED THREE-DIMENSIONAL GROUNDWATER FLOW MODEL

The assumed geographic setting of the local hydrogeological model for the present study covers a 10 km x 9 km area of the Whiteshell Research Area (Figure 1) and extends to a depth of 1.5 km. As in the EIS case study the background rock for the hydrogeological model was assumed to be an equivalent porous media and was divided into three horizontal layers. The top two layers (from ground surface to 300 m depth) were assigned anisotropic permeabilities, with vertical permeability equal to five times the horizontal permeability to represent the average effect of systematic subvertical fractures in this portion of the rock mass. Major fracture zones were included as discrete features in the model. These fracture

zones were assumed to have a uniform thickness of 20 m and were modelled as equivalent porous media with 10^{-13} m^2 longitudinal permeability. The geometry of the model near the vault is shown in Figure 2 and the finite element mesh is identical to the mesh used in the EIS case study (Davison et al. 1994b). The boundary conditions applied were fixed head equal to the topography on the top surface and no-flow on the sides and bottom. To verify that the boundaries had no effect on the groundwater flow conditions in the region of the vault, a second model was run where hydrostatic heads were assigned to the sides of the model. There was little effect on the hydraulic head distribution in the region of the vault. Thus, no regional groundwater flow modelling was performed for this study, contrary to the approach followed in developing the geosphere model for the EIS case study (Davison et al. 1994b).

The major differences between the geosphere model used in this present study and that used in the original EIS case study are:

1. The hydrogeological properties of the layer of rock immediately surrounding the waste emplacement areas of the vault (rock layer 3) are assumed to be identical to those of rock layer 2 with one exception; we assumed there was no vertical anisotropy in the permeability of layer 3.

   The vertical anisotropy in rock layers 1 and 2 were introduced in the EIS case study to account for the subvertical fracturing observed in shallow portions of the rock mass at the WRA. For this study we assigned a uniform permeability of 10^{-17} m^2 to rock layer 3 (from 300 m depth to 1500 m depth). In the EIS case study we had assumed a permeability of 10^{-19} m^2 for this layer. We have encountered rock with a permeability of 10^{-17} m^2 at 500 m depth at our East Bull Lake (EBL) and Atikokan (ATK) research areas, although the permeability decreases to 10^{-19} m^2 by 900 m depth at these two research areas (Figure 3). The permeability value of 10^{-17} m^2 is similar to the permeability assumed for the rock at depths of 300 m to 600 m in Finnish and Swedish assessments of nuclear waste disposal in crystalline rocks of the Fennoscandian Shield (SKI 1991; TVO, 1992a; TVO 1992b; Elert et al. 1992; SKB 1992) (Figure 3).

   In addition, the effects of a "dual-porosity medium" were considered in this study by assuming that the permeability of the rock layers in the geosphere model was due to the effects of discrete fractures through the rock layers. The effective porosity assigned to the rock layers in some of the runs with this model is significantly smaller than the total porosity of the unfractured rock matrix (3-5 x 10^{-3}). A range of effective porosities of 10^{-3} to 10^{-5} was chosen to represent these discrete fracture effects. This is the same range of effective porosity values considered for the rock mass in the Swedish assessments of nuclear fuel waste disposal in crystalline rocks of the Fennoscandian Shield (SKI 1991; Elert et al. 1992; SKB, 1992). Our own recent analysis of some of the transient hydraulic head drawdown data for the upper fractured rock domain at the URL site (to a depth of 130 m) has also indicated a hydraulically-effective porosity of about 10^{-4} for this type of rock domain (Frost 1996).

   In addition to these changes it also was decided to modify the hydrogeologic characteristics of the discrete fracture zones in this model to take account of new information on the transport properties of these types of fracture zones. The effective porosity of the fracture zones was decreased to 10^{-2} to be consistent with recent field evidence from large scale groundwater tracer tests in similar fracture zones at the WRA and URL site (Frost and Davison 1995; and Frost et al. 1995a,b,c). The EIS geosphere

model assumed these fracture zones had an effective porosity of 10^{-1} (Davison et al. 1994b).

2. The natural geothermal gradient observed in the rock at the URL (Drury 1982) and an in-room emplacement waste heat generation term (Baumgartner et al. 1995b) have been included in this study.

3. Waste emplacement areas of the vault are located both to the right of fracture zone LD1 (above LD1) as well as to the left of LD1 (below LD1) in this study (Figure 2). In the EIS case study we assumed the waste emplacement areas of the vault were only located below LD1 although our sensitivity analyses had examined the effects of locating a portion of the vault above LD1 (Davison et al. 1994b). As in the EIS case study, we have assumed that the waste emplacement areas of the disposal vault are located at least 50 m away from the nearest major fracture zone, LD1.

Other relevant geosphere model properties were derived from either field and laboratory work or literature review. They were:

1. transport properties - dispersivities along the various pathways through the geosphere, free-water diffusion coefficients and tortuosity factors;

2. mineralogy and groundwater chemistry - groundwater salinity (total dissolved solids) at different locations along the geosphere pathways, location of the groundwater redox divide (the position along a flow path at which the redox potential of the groundwater changes from oxidizing to reducing), mineral content along the different pathways through the geosphere, and radionuclide retardation coefficients that relate to the groundwater salinity and redox condition of the groundwater and the mineral content of the flow paths; and

3. miscellaneous properties such as the thickness of sediment and overburden at the discharge locations in the biosphere and the radius of the casing of the water supply well in fracture zone LD1.

In many cases, the values of these properties for this study were not changed from those used in the EIS case study. In some cases, however, they were either changed or needed to be justified in the context of this particular study. We note these in the following report.

3. SIMULATIONS USING DETAILED GROUNDWATER FLOW MODEL

Three groundwater flow model cases were investigated in detail as part of this study: Case 1 is the groundwater flow model used in the original EIS case study (Davison et al. 1994b and Chan et al. 1995); Case 2 has similar properties to Case 1 except rock layer 3 has the permeability increased by two orders of magnitude to 10^{-17} m^2 and the porosity increased slightly from 3×10^{-3} to 4×10^{-3}; in Case 3 we assumed the flow in the rock layers occurred within networks of thin fractures. The rock layers in Case 3 were assigned the same permeabilities at those of Case 2 but were assigned much lower effective porosities to represent these conditions (10^{-5}). The properties used in these three cases are summarized in Table 1.

Note that for the following sections there is no simulation of a pumping well in fracture zone LD1 unless otherwise stated.

3.1 GROUNDWATER TRAVEL TIMES - ISOTHERMAL CONDITIONS

The groundwater travel times from the vault to the biosphere for isothermal simulations are illustrated in Figure 4. These show a substantial reduction in travel times going from Case 1 to Case 2 to Case 3.

For advective groundwater flow pathways starting in that portion of the vault to the right of the vault/fracture zone (LD1) intersection (i.e. above LD1), the minimum travel time from the vault to the biosphere for Case 1 is 135,000 years, for Case 2 the minimum travel time is 3,600 years, and for Case 3 the minimum travel time is 110 years.

For advective groundwater flow pathways starting in the portion of the vault to the left of the vault/fracture zone (LD1) intersection (i.e. below LD1), the minimum travel time from the vault to the biosphere for Case 1 is 4.5×10^6 years, for Case 2 the minimum travel time is 52,000 years, and for Case 3 the minimum travel time is 170 years.

3.2 INFERRED GROUNDWATER AGES

The approximate groundwater ages of water moving through the location of the vault were calculated by reversing the groundwater flow field in the models and tracking particles back from the vault horizon to their recharge locations at the ground surface (Figure 5). Isothermal conditions were assumed. For Case 1 (Figure 5, histogram a) the minimum groundwater age at the location of the vault horizon in the flow field was calculated to be about one million years. For Case 2 (Figure 5, histogram b) the minimum groundwater age at the vault location was about 15,000 years. The minimum groundwater age was calculated to be about 80 years at the location of the vault for Case 3 (Figure 5, histogram c). Although this latter case represents a relatively short period of time for recharging, oxygenated surface waters to penetrate the rock to vault depths, it is still considered sufficiently long for all the groundwater reaching the depth of the hypothetical vault (500 m) to have evolved to a reducing environment (Gascoyne et al. 1995).

3.3 GEOTHERMAL AND VAULT HEATING EFFECTS

The effect of a natural geothermal gradient in the rock of the model was investigated by including in the simulation the geothermal gradient measured at the URL (Drury 1982). This effect increased the rate of groundwater flow away from the vault and reduced the minimum travel time along advective groundwater flow pathways from the vault to the biosphere by 15%. For instance, for pathways from the portion of the vault above LD1 the travel times were reduced from 3,600 years to approximately 3100 years for the conditions of Case 2 and from 110 years to 95 years for the conditions of Case 3.

The inclusion of the effects of the heat generated by the nuclear fuel waste in the vault (the thermal gradient imposed by the heat generated by decay of radionuclides in the used fuel) (Baumgartner et al. 1995) further reduced the minimum travel time along advective pathways in the geosphere to 2,570 years for Case 2. The minimum travel time was not significantly reduced for Case 3 when vault heating was accounted for. The travel time histograms along various geosphere pathways from the vault for the subcases accounting for the effects of the natural geothermal gradient in the rock and the effects of

radiogenic heat from the wastes are illustrated in Figure 6. The first two histograms labelled 1a and 1b are for Case 2. The two histograms labelled 2a and 2b are for Case 3.

Figures 7 to 10 show the hydraulic head distributions in the vicinity of the vault for the Case 1 model (Figure 7) and the different variations of the Case 2 model: assuming isothermal conditions (Figure 8); natural geothermal gradient (Figure 9); and the analysis of natural geothermal gradient plus the maximum effects of waste heat (Figure 10). The head distributions for Case 1 (Figure 7) and the isothermal Case 2 (Figure 8) are very similar except that the influence of the vertical fracture zone V1 is reduced in Case 2 as a result of the reduction in the permeability contrast between the rock matrix in layer 3 and the fracture zone. By comparing Figures 8 and 9, it can be seen that the effect of the natural geothermal gradient in the rock mass is significant. Although not shown in these figures, it is also important to note that the head distributions were not changed as a result of decreasing the porosity of the rock layers from 4×10^{-3} to 10^{-5} (Case 2 and Case 3).

Particle tracking was also performed to examine if there were any changes to the advective flow field within fracture zone LD1 caused by changing the hydraulic properties of rock layer 3. The analyses were performed for the isothermal Cases 1 and 2. As expected, changing the permeability properties of rock layer 3 from 10^{-19} m^2 to 10^{-17} m^2 did not effect the advective flow paths within fracture zone LD1 (Figure 11). As well, the flow field within fracture zone LD1 was not affected by the change in porosity of the rock layers introduced in Case 3 (i.e. from 4×10^{-3} to 10^{-5}).

Figure 12 shows particle tracks of the advective flow paths from the vault for isothermal Cases 1 and 2. In Case 2 rock layers 2 and 3 effectively have the same hydraulic properties (although there is a small component of vertical anisotropy in the permeability of layer 2). Thus the flow paths from the vault do not refract at the rock layer boundaries in Case 2 as they do in Case 1, rather they continue on until they reach one of the major fracture zones. By examining the particle tracks for the cases that considered the effects of a natural geothermal gradient, and a natural geothermal gradient plus waste heat (Figure 13a and 13b), it can be seen that there are minimal changes between these two cases. It should also be noted in the pattern of particle tracks shown in Figures 12 and 13 that transport up fracture zone LD0 becomes an important additional pathway for advective transport from the vault to the surface when the permeability of rock layer 3 is increased to 10^{-17} m^2. In Case 1, when the permeability of rock layer 3 was 10^{-19} m^2, fracture zone LD0 did not constitute a significant advective pathway from the vault to the groundsurface (Figure 12).

As with the geosphere model in the EIS case study, the advective flow pathways from the position of the hypothetical vault emerge (discharge) at ground surface at two regions in Boggy Creek and also into the Pinawa Channel. Figure 14 shows the surface discharge exit locations for particles started in the vault for: a) the isothermal Case 1; b) the isothermal Case 2; c) the geothermal gradient Case 2; and d) the geothermal gradient plus waste heat Case 2. In all the Case 2 examples, the influence of advective flow up fracture zone LD0 can be seen in the increase in size of the area where pathways from LD0 emerge at surface. This area is referred to as the Boggy Creek North discharge area. Pathways emerging in this discharge area have followed flow paths within fracture LD0 for much of their travel length. The size of the area of emergence of pathways in the Boggy Creek South discharge area does not change significantly, however the shape of the area of emergence does. The size of the area of emergence of pathways in the Pinawa Channel discharge area is only reduced when the waste heat is applied.

3.4 MAXIMUM THERMAL EFFECTS ON GEOSPHERE PATHWAYS

Since GEONET cannot handle time-dependent velocity fields, an analysis was performed with the MOTIF model to determine the future time at which the groundwater velocity in the vicinity of the vault would be at a maximum, due to the transient effects of radiogenic heating on the advective groundwater flow field. This time was found to be 4400 years and it was chosen as the base case for all subsequent analysis. When we assumed that these thermally-accelerated groundwater velocities were constant over the entire modelling time, the minimum travel time for Case 2 conditions was reduced to 2570 years (from 3100 years for Case 2 without thermal effects due to radiogenic heat). For the conditions of the Case 3 model, the minimum travel time for advective transport from the vault to surface discharge areas was reduced to 70 years when the thermally accelerated flow field was used, compared to 95 years if these effects were not included. This latter case yielded the shortest advective travel times through the geosphere of all the cases we examined and we considered it to be the most conservative for subsequent geosphere modelling purposes.

The travel time histograms for particles started in the vault for the geothermal gradient and waste heat maximum velocity field subcase are also illustrated in Figure 6. The histogram labelled 1c is for Case 2 and histogram labelled 2c is for Case 3. Figure 10 shows the hydraulic head distribution in the vicinity of the vault for the case representing conditions under the combined influence of a natural geothermal gradient and the maximum waste heat effect. When compared to Figure 9 the only hydraulic head changes are seen in the portion of the model under Boggy Creek where the hydraulic head gradient has been reduced.

Although it is not evident on the hydraulic head plots, there are significant differences in the near-field patterns of geosphere pathways when the maximum thermal effect is considered. The high vault heat output of this maximum thermal effect induces a flow pattern that causes much faster movement to the fracture zones in the rock layers above the vault for pathways originating over the entire extent of the vault. In the other cases, with no or lesser vault heat, a small number of flow paths from the vault are actually directed downward, away from fracture zone LD1, before they bend around in the direction of fracture zone LD1. Pathways from these locations of the vault are aligned directly towards the fracture zone when the maximum vault heat effect is considered. Figure 13 illustrates this and Figure 14e also shows the discharge locations of the pathways from the vault for this case.

3.5 EFFECTS OF A WATER SUPPLY WELL

As in the previous EIS case study (Davison et al. 1994b; Chan and Nakka, 1994), the effects of a domestic groundwater-supply well drawing water continuously from fracture zone LD1 were considered in this study. The well was assumed to intersect LD1 at various depths up to a maximum of 200 m. This was the greatest depth at which a well could intersect fracture zone LD1 without first intersecting the shallower fracture zone, LD2 (Figure 2). This was considered to be the deepest well that would conceivably be drilled in such a setting for water supply purposes. The well pumping rate was varied from zero to the maximum well capacity for each specific well depth, but was assumed to be constant in time in all simulations. As with the previous EIS case study, this analysis showed that:

(1) pumping from the well in LD1 reduced the area over which pathways from the vault emerged at the Boggy Creek South surface discharge area in the biosphere. The effects on pathways emerging at the other surface discharge areas were much smaller. The pumping effects were especially noticeable for deeper wells with higher pumping rates (Figure 15); and

(2) depending on well depth and pumping rate, the minimum groundwater travel times along pathways from the vault to surface discharge areas could be reduced to 15%, or increased by 200% to 300% of the no-well values. This depended on where the pathway originated in the vault.

4. DEVELOPMENT OF GEONET

From the detailed modelling with MOTIF described above, various quantities were derived for use in the SYVAC geosphere model, GEONET. These quantities define and characterize the 3-D network of transport pathways from the vault to the biosphere through this hypothetical permeable geosphere and they take account of vault-induced thermal effects as well as the effects of a well pumping water from LD1. The quantities include: the nodal coordinates of the pathways from the vault through the geosphere to their discharge locations in the biosphere; the segments of the pathways and their physical and chemical property classes; the segment permeabilities, porosities and dispersivities; and, the nodal hydraulic heads and temperatures. In addition, a number of empirical relationships were also developed to account for the thermal and pumping effects on the transport pathways from the vault. One such empirical relationship describes the reduction of the areas over which pathways from the vault emerge at the Boggy Creek South discharge area as a function of well depth and pumping rate.

The Empirical Vault Head Equations that were used in the EIS case study to describe the effects of a well on the transport network (Davison et al. 1994b; Chan and Nakka, 1994) were not applicable to the geosphere model of this case and needed to be replaced. As a result an empirical equation was developed to account for the drawdown effects of the pumping well. This was done for each node outside fracture zone LD1 which could be potentially affected by the well drawdown. These new empirical equations are described in Section 4.3.

The MOTIF simulations used to define the GEONET network and parameters can take account of the natural geothermal gradient in the rock and the transient effects of vault heating. However GEONET is unable to handle time-varying parameter values. Therefore the decision was made to assume that the hydraulic head and temperature distribution for the entire GEONET analysis period was equal to the hydraulic head and temperature distribution at that time at which the thermal effect of the vault on the geosphere pathways was at its maximum, ~4400 years. The well effects are superimposed on this distribution using the empirical relations and other equations described later in Section 4.3.

4.1 DETERMINING THE NETWORK GEOMETRY

In order to determine the preliminary geometry of the 3-D network of geosphere pathways from the vault to the biosphere for a vault located at 500 m depth in this hypothetical geosphere, we first used the advective groundwater flow velocity field from a MOTIF simulation without a well. 504 particles were distributed uniformly across the surface of the new hypothetical disposal vault developed for this case (Baumgartner et al. 1996) and tracked through the groundwater flow field in the permeable geosphere to discharge areas at groundsurface using TRACK3D. We determined if advection dominated the transport process by calculating the Peclet number (Freeze and Cherry 1979) for each flow path in the geosphere. For all the flow paths, the Peclet number was found to be greater than five and was frequently greater than ten. Thus, unlike the previous geosphere model of the EIS case study no diffusion paths needed to be incorporated into this geosphere model. The GEONET pathways were subsequently constructed to

closely match the geometry of the three-dimensional advective groundwater flow paths from the vault to the biosphere as determined from this particle tracking.

Each GEONET pathway is composed of a number of connected linear segments. In locating the segments care was taken to ensure that each segment lies only within a single material property zone and that the groundwater velocity does not vary excessively over the volume of rock represented by the segment. Each segment was assigned a set of physical properties and a set of chemical properties. The physical and chemical property sets are associated with the rock/fracture zone in which the segment is located. For instance rock layers 1, 2 and 3 of the hypothetical site model have different physical and chemical properties, and the fracture zones also have different properties.

Once this preliminary network of geosphere transport pathways had been developed, the suitability of the network for representing flow within the geosphere in the presence of a pumping well in fracture zone LD1 was checked. MOTIF simulations were performed to simulate wells with depths of 30 m, 100 m and 200 m in LD1 and with pumping rates ranging from 120 m^3/a to the maximum well capacity (depends on depth of well). For the 30 m deep well, the alteration of the geosphere pathways from the vault to discharge areas in the biosphere was minimal. For the 100 m deep well, some transport pathways that originated near the left edge of the vault (below LD1) were captured by the well. An additional transport segment was introduced into GEONET to account for this effect. When the 200 m deep well cases were examined, there were significant perturbations to the geometry of the transport paths from the vault to the biosphere. These large perturbations were caused by the fact that the 200 m deep well penetrates LD1 below the depth of the interface between rock layer 1 and rock layer 2. In this situation advective groundwater flow pathways from the vault are diverted directly to the well location rather than travelling vertically through rock layers 2 and 3. This complicates the pathways network substantially. In order to expedite creation of a usable pathways network for GEONET it was decided to not incorporate the effects of wells deeper than 100 m in the GEONET model for this study. It should be noted that wells deeper than 100 m represent only a small percentage (about 8% (9 out of 112)) of the domestic water supply wells currently existing in the crystalline rocks of the region surrounding and including the WRA (Stevenson 1995). Figure 16a shows the preliminary (no well) GEONET network of pathways from the vault to discharge locations at surface. The network segments are superimposed on the MOTIF pathways (particle tracks) to illustrate how they were determined. Figure 16b shows the network of pathways which accounts for the effects of a 10,000 m^3/a 100 m deep well in LD1. The final geometry of pathways we incorporated into GEONET is illustrated in Figure 17. This figure also shows the locations of the 24 source nodes that represent different portions of the plane of the disposal vault at 500 m depth and the 5 nodes where the geosphere pathways emerge into surface discharge areas at the biosphere, including at a well in fracture zone LD1.

4.2 NETWORK PARAMETERS

Once the GEONET pathways network had been established, the necessary parameters required for GEONET simulations were determined. Tables 2 to 9 list the nodal coordinates of the transport pathways from the disposal vault to the biosphere, the different segments of these pathways and their physical and chemical property classes, the segment permeabilities, porosities and dispersivities, the hydraulic heads and temperatures at the nodes of the transport paths and the size of the areas where the pathways emerge at the biosphere. The sorption data has been documented in Vandergraaf et al. 1992 and Ticknor and Vandergraaf 1996.

The range for dispersivities were chosen to be 0.01L to 0.9L for transport segments in the rock layers and 0.01L to 0.25L for segments in the fracture zones, where L is the length of the segment. The dispersivity

data compiled by Gelhar et al. (1992) was used to develop the relationship for the pathways through the different rock layers in the model. The field tracer test data of Frost and Davison (1995) and Frost et al. (1995a,b, and c) for groundwater tracer tests in fracture zones at the WRA like LD1 was used to develop the relationship for the fracture zones in the model.

4.3 THE WELL PARAMETERS

Accounting for the influences of water supply wells of various depths and pumping rates on the geometry of the geosphere transport paths and their velocities is crucial to the proper simulation capabilities of the GEONET model. We have developed special well parameters to account for these influences.

One of the first steps in developing the well parameters for this study was to determine if the analytical well models we had used for the previous EIS case study (Davison et al. 1994b; Chan and Nakka, 1994) were appropriate for this study. A primary assumption in the previous analytical model was that the aquifer (fracture zone LD1) in which the well is located is effectively non-leaky. Because the permeability properties of rock layer 3 had changed significantly for this study (from 10^{-19} m^2 to 10^{-17} m^2) we needed to determine whether the rock surrounding LD1 had sufficiently low permeability in this new model to assume a non-leaky aquifer model would apply. In order to accomplish this we examined the amount of flux leaking from the adjacent rock into fracture zone LD1 in those MOTIF simulations of the various well depths and demands. The leakage rate from the adjacent rock layers into the well aquifer (LD1) was found to be very small in all these simulations. Therefore, we concluded that the assumption of a non-leaky aquifer would be applicable to the conditions of this new study and that we could use the same analytical well model as we had used in the previous EIS case study (Davison et al. 1994b; Chan and Nakka, 1994).

The basic well parameters for this geosphere model were assigned the same values as those used in the previous EIS case study except for the value chosen for the maximum well depth. As we stated previously, this GEONET network is only applicable for wells in LD1 with depths of 100 m or less whereas the geosphere model of the EIS case study could represent wells to a depth of 200 m in LD1. Deeper wells into LD1 or wells into other fracture zones are not represented by the GEONET network we have specified for this study.

The particle tracking results were used to determine the shape of the flow pathways from the vault (Figure 12) and also within fracture zone, LD1 (Figure 11). The pathways moving up fracture LD1 did not change significantly between this study and the previous EIS case study. Particle tracks that trace the pathways from the left-hand side of the vault (below LD1) travel generally upwards or subparallel to fracture zone LD1. (Figure 13) Those paths that enter LD1 do so at depths of about 150 to 200 m below ground surface.

In developing the GEONET transport network of pathways in LD1 we also define a capture line for the well. Transport paths within this line can be captured by a pumping well drawing groundwater from LD1. This capture line must lie between the location where the pathways enter LD1 and the location of the drawdown node associated with the deepest well in LD1. For this transport network, the drawdown nodes were located in LD1 within 20 m of the actual well location and the well depth was restricted to a maximum depth of 100 m. Thus, the well capture line was located at 110 m below ground surface in LD1. This capture line contains a total of 6 capture nodes. Portions of the advective transport pathways from the vault that move up LD1 are assigned to those network segments that originate at one of these capture nodes and connect to the well.

Three of the nodes represent portions of the pathways that originate from the right-hand side of the vault (above LD1). These are pathways that enter fracture zone LD1 below the vault level and travel more than 1400 m in LD1. These pathways converge with the natural flow field in the fracture zone and they occur in a 380 m wide portion of LD1 at the elevation of the well capture line in LD1.

The other three capture nodes represent pathways that originate from the left-hand side of the vault (below LD1). These pathways enter fracture zone LD1 closer to the well capture line. These pathways have not converged as strongly, since they have travelled largely outside the fracture zone and they occupy a width of about 1240 m in LD1 when they arrive at the well capture line. In addition, these three capture nodes are not symmetrically placed about the well centre line. Pathways originating on the NE side of the vault remain more diffuse in LD1 and remain further from the centre line of the well. Two portions of the pathways that originate from the left-hand side and right-hand side of the vault move up the same, central part of the flow field in fracture zone LD1.

A summary of the capture widths assigned to the transport segments originating at the well capture nodes in fracture zone LD1 is given in Table 10 which account for these flow effects within fracture zone LD1. This is also illustrated in Figure 18.

In addition to these parameters, a number of empirical relationships were developed to account for the effects of the pumping well in LD1 on the geosphere pathways. The first describes the reduction in the size of the discharge areas where the pathways emerge at groundsurface as a function of well depth and pumping rate. For the wells investigated, only the pathways emerging at the Boggy Creek South discharge area are affected (Figure 15). The relationship which describes this is represented by the following equation:

$$A_d = \exp^{-1.85 \times 10^{-4} Q_w} \quad (1)$$

where

A_d = normalized discharge area = A/A_o
- where A = the area of Boggy Creek South where pathways from the vault emerge in the presence of a well in LD1 supplying demand Q_w and
- A_o = the area of Boggy Creek South where pathways from the vault emerge in the presence of no well in LD1

Q_w = well demand.

Figure 19 illustrates the effect on the emergence of pathways from the vault at the Boggy Creek South discharge area as a function of well demand. The size of the area of this discharge is independent of well depth.

In the previous EIS case study, the effects of the pumping well in fracture zone LD1 on nodes outside LD1 were calculated by the Empirical Vault Head Equations (Davison et al. 1994b). In this present study, this approach was not applicable since transport segments starting at the vault do not lead directly into fracture zone LD1. The approach used in this study was to determine an empirical equation for the hydraulic head change for each node outside the LD1 which could be potentially affected by the well

drawdown. It was determined from MOTIF modelling of these effects that the head change for each of these nodes could be expressed by an equation of the form:

$$*h_i = A_n Q_w (D_w/100^2) \quad (2)$$

where

$*h_i$ = head change (m)
Q_w = Well demand (m^3/a)
D_w = Well depth (m)
A_n = Node specific constant (a/m^4)

The values of the constant A_n are listed in Table 11. Figure 20 plots the drawdowns at the nodes affected by the well in LD1 as calculated using the empirical equation versus those obtained from the MOTIF simulations for both the 30 m and 100 m deep wells in fracture zone LD1.

5. SUMMARY AND CONCLUSIONS

The geosphere model we have developed for this study is hypothetical because it does not represent conditions that we have encountered at any of our geologic research areas on the Canadian Shield. The geometry of the main hydrogeologic features of the model: surface topography; depths of different rock domains; location of major fracture zones; and the location of the disposal vault horizon (500 m) is identical to that used for the EIS case study. However, the geosphere model for this study assumes much higher permeability and lower porosity for the rock domain surrounding the waste emplacement areas of the disposal than the conditions used in the EIS case study. In addition, the vault horizon is partitioned such that some of the vault is situated above a low dipping fracture zone as well as below the fracture zone. As a result, transport from the vault through the geosphere is dominated by advection in groundwater flowing through interconnected fracture networks in the rock rather than by diffusion through a volume of sparsely fractured, very low permeability rock which was the case in the geosphere model for the EIS case study. The travel times along groundwater flow paths from the disposal vault to surface discharge areas are 1000 to 10,000 times shorter in this geosphere model than in the geosphere model used for the EIS case study.

We used the same approach in developing a model of the transport pathways from the disposal vault to discharge locations at groundsurface for this hypothetical set of geosphere conditions as we used in the EIS case study. The MOTIF finite element code was used to simulate groundwater flow through a 3-D model of the vault and hydrogeologic conditions. The effects of natural geothermal heat and vault-induced heating were also accounted for in the groundwater flow model. A particle tracking code (TRACK3D) was used to trace the advective groundwater flow paths from the hypothetical disposal vault to discharge areas at groundsurface. Under the conditions of the maximum vault heating effects and the lowest values of the range of rock porosity, the shortest advective travel time from the vault to groundsurface was about 70 years.

In addition, the effects of a domestic water supply well drawing groundwater from a low dipping fracture zone passing through the depth horizon of the vault were also investigated with the MOTIF groundwater flow model.

A pathways network model (GEONET) was developed to represent the advective flow paths from the vault to surface discharge locations in the biosphere through this permeable geosphere. GEONET was also developed to be able to represent the effects on the geosphere pathways of a well drawing groundwater from a depth of up to 100 m in the fracture zone. Two empirical relationships were incorporated into GEONET to account for the pumping effects on the advective transport pathways from the vault to the biosphere. One defines the size of the area at groundsurface where pathways from the vault emerge, the other defines to what extent the pathways from the vault are captured by the pumping well.

ACKNOWLEDGEMENTS

The Canadian Nuclear Fuel Waste Management Program is funded jointly by AECL and Ontario Hydro under the auspices of the CANDU Owners Group.

REFERENCES

AECB (Atomic Energy Control Board). 1987. Regulatory policy statement. Regulatory objectives, requirements and guidelines for the disposal of radioactive wastes — long-term aspects. Atomic Energy Control Board Regulatory Document R-104, 1987 June 5.

AECL (Atomic Energy of Canada Limited). 1994a. Environmental impact statement on the concept for disposal of Canada's nuclear fuel waste. Atomic Energy of Canada Limited Report, AECL-10711, COG-93-1. Available in French and English.

AECL (Atomic Energy of Canada Limited). 1994b. Summary of the environmental impact statement on the concept for disposal of Canada's nuclear fuel waste. Atomic Energy of Canada Limited Report, AECL-10721, COG-93-11. Available in French and English.

Baumgartner, P., D.M. Bilinsky, Y. Ates, R.S. Read, J.L. Crosthwaite, and D.A. Dixon. 1996. Engineering for a disposal facility using the in-room emplacement method. Atomic Energy of Canada Limited Report, AECL-11595, COG-96-223.

Chan, T. and B.W. Nakka. 1994. A two-dimensional analytical well model with applications to groundwater flow and convective transport modelling in the geosphere. Atomic Energy of Canada Limited Report, AECL-10880, COG-93-215.

Chan, T., B.W. Nakka, P.A. O'Connor, D.U. Ophori, N.W. Scheier and F.W. Stanchell. 1994. Thermohydrogeological modelling of the Whiteshell Research Area. Atomic Energy of Canada Limited Report, AECL-10947, COG-93-368.

Davis, P.A., R. Zach, M.E. Stephens, B.D. Amiro, G.A. Bird, J.A.K. Reid, M.I. Sheppard, S.C. Sheppard and M. Stephenson. 1993. The disposal of Canada's nuclear fuel waste: The biosphere model, BIOTRAC, for postclosure assessment. Atomic Energy of Canada Limited Report, AECL-10720, COG-93-10.

Davison, C.C., A. Brown, R.A. Everitt, M. Gascoyne, E.T. Kozak, G.S. Lodha, C.D. Martin, N.M. Soonawala, D.R. Stevenson, G.A. Thorne and S.H. Whitaker. 1994a. The disposal of Canada's nuclear fuel waste: Site screening and site evaluation technology. Atomic Energy of Canada Limited Report, AECL-10713, COG-93-3.

Davison, C.C., T. Chan, A. Brown, M. Gascoyne, D.C. Kamineni, G.S. Lodha, T.W. Melnyk, B.W. Nakka, P.A. O'Connor, D.U. Ophori, N.W. Scheier, N.M. Soonawala, F.W. Stanchell, D.R. Stevenson, G.A. Thorne, T.T. Vandergraaf, P. Vilks and S.H. Whitaker. 1994b. The disposal of Canada's nuclear fuel waste: The geosphere model for postclosure assessment. Atomic Energy of Canada Limited Report, AECL-10719, COG-93-9.

Drury, M.J. 1982. Geothermal logging of URL boreholes, 1981. Earth Physics Branch, Energy, Mines and Resources Canada Internal Report, 82-2.

Elert, M., I. Neretnicks, N. Kjellbert and A. Ström. 1992. Descriptions of transport mechanisms and pathways in the far field of a KBS-3 type repository. SKB Technical Report 92-09.

Freeze, R.A. and J.A. Cherry. 1979. Groundwater. Prentice-Hall Inc., Englewood Cliffs, N.J., 604.

Frost, L.H. and C.C. Davison. 1995. Summary of the fracture zone 3 groundwater tracer test programs at the Underground Research Laboratory. Atomic Energy of Canada Limited Technical Record, TR-617, COG-95-89.

Frost, L.H., N.W. Scheier and C.C. Davison. 1995a. Two-well radioactive tracer experiment in a major fracture zone in granite. Atomic Energy of Canada Limited Technical Record, TR-671.

Frost, L.H., N.W. Scheier and C.C. Davison. 1995b. Transport properties in highly fractured rock experiment: Phase 1 tracer tests in fracture zone 2. Atomic Energy of Canada Limited Technical Record, TR-685, COG-95-198.

Frost, L.H., N.W. Scheier and C.C. Davison. 1995c. Transport properties in highly fractured rock experiment: Phase 2 tracer tests in fracture zone 2. Atomic Energy of Canada Limited Technical Record, TR-685, COG-95-198.

Gascoyne, M., J.D. Ross and R.L. Watson. 1995. Hydrogeochemical and geochemical data for the alternate assessment assessment case study for nuclear fuel waste disposal in Canada. Atomic Energy of Canada Limited Technical Record, TR-720, COG-95-543.

Goodwin, B.W., D.B. McConnell, T.H. Andres, W.C. Hajas, D.M. LeNeveu, T.W. Melnyk, G.R. Sherman, M.E. Stephens, J.G. Szekely, P.C. Bera, C.M. Cosgrove, K.D. Dougan, S.B. Keeling, C.I. Kitson, B.C. Kummen, S.E. Oliver, K. Witzke, L. Wojciechowski and A.G. Wikjord. 1994. The disposal of Canada's nuclear fuel waste: Postclosure assessment of a reference system. Atomic Energy of Canada Limited Report, AECL-10717, COG-93-7.

Goodwin, B.W., T.H. Andres, W.C. Hajas, D.M. LeNeveu, T.W. Melnyk, J.G. Szekely, A.G. Wikjord, D.C. Donahue, S.B. Keeling, C.I. Kitson, S.E. Oliver, K. Witzke and L. Wojciechowski. 1996. The disposal of Canada's nuclear fuel waste: A study of postclosure safety of in-room emplacement of used CANDU fuel in copper containers in permeable plutonic rock. Volume 5: Radiological Assessment. Atomic Energy of Canada Limited Report, AECL-11494-5, COG-95-552-5.

Greber, M.A., E.R. Frech and J.A.R. Hillier. 1994. The disposal of Canada's nuclear fuel waste: Public involvement and social aspects. Atomic Energy of Canada Limited Report, AECL-10712, COG-93-2.

Grondin, L., K. Johansen, W.C. Cheng, M. Fearn-Duffy, C.R. Frost, T.F. Kempe, J. Lockhart-Grace, M. Paez Victor, H.E. Reid, S.B. Russell, C.H. Ulster, J.E. Villagran and M. Zeya. 1994. The disposal of Canada's nuclear fuel waste: Preclosure assessment of a conceptual system. Ontario Hydro Report N-03784-940010 (UFMED), COG-93-6.

ICRP (International Commission on Radiological Protection). 1991a. 1990 recommendations of the International Commission on Radiological Protection. Annals of the ICRP 21(1-3) (ICRP Publication 60).

ICRP (International Commission on Radiological Protection). 1991b. Annual limits on intake of radionuclides by workers based on the 1990 recommendations. Annals of the ICRP 21(4) (ICRP Publication 61).

Johnson, L.H., J.C. Tait, D.W. Shoesmith, J.L. Crosthwaite and M.N. Gray. 1994a. The disposal of Canada's nuclear fuel waste: Engineered barriers alternatives. Atomic Energy of Canada Limited Report, AECL-10718, COG-93-8.

Johnson, L.H., D.M. LeNeveu, D.W. Shoesmith, D.W. Oscarson, M.N. Gray, R.J. Lemire and N. Garisto. 1994b. The disposal of Canada's nuclear fuel waste: The vault model for postclosure assessment. Atomic Energy of Canada Limited Report, AECL-10714, COG-93-4.

Johnson, L.H., D.M. LeNeveu, D.W. Shoesmith, F. King, M. Kolar, D.W. Oscarson, S. Sunder, C. Onofrei and J.L. Crosthwaite. 1996. The disposal of Canada's nuclear fuel waste: A study of postclosure safety of in-room emplacement of used CANDU fuel in copper containers in permeable plutonic rock. Volume 2: Vault Model. Atomic Energy of Canada Limited Report, AECL-11494-2, COG-95-552-2.

Nakka, B.W. and T. Chan. 1994. A particle-tracking code (TRACK3D) for convective solute transport modelling in the geosphere: description and user's manual. Atomic Energy of Canada Limited Report, AECL-10881, COG-93-216.

Ophori, D.U., T. Chan and F.W. Stanchell. 1994. Sensitivity analysis of the effects of a domestic water supply well in the Whiteshell Research Area. Atomic Energy of Canada Limited Technical Record, TR-619, COG-93-202.

Ophori, D.U., D.R. Stevenson, M. Gascoyne, A. Brown, C.C. Davison, T. Chan and F.W. Stanchell. 1995. Revised model of regional groundwater flow of the Whiteshell Research Area: Summary. Atomic Energy of Canada Limited Report, AECL-11286, COG-95-115.

Ophori, D.U., A. Brown, T. Chan, C.C. Davison, M. Gascoyne, N.W. Scheier, F.W. Stanchell and D.R. Stevenson. 1996. Revised model of regional groundwater flow in the Whiteshell Research Area. Atomic Energy of Canada Limited Report, AECL-11435, COG-95-443.

Simmons, G.R. and P. Baumgartner. 1994. The disposal of Canada's nuclear fuel waste. Engineering for a disposal facility. Atomic Energy of Canada Limited Report, AECL-10715, COG-93-5.

SKB. 1992. SKB 91: Final disposal of spent nuclear fuel. Importance of Bedrock for Safety. SKB Technical Report 92-20.

SKI. 1991. SKI Project-90, Volume 1. SKI Technical Report 91:23.

Stevenson, D.R. 1995. Number of hard rock wells deeper than 100 m in the WRA and surrounding area. Personal communication.

Stevenson, D.R., A. Brown, C.C. Davison, M. Gascoyne, R.G. McGregor, D.U. Ophori, N.W. Scheier, F.W. Stanchell, G.A. Thorne and D.K. Tomsons. 1995. A revised conceptual hydrogeologic model of a crystalline rock environment, Whiteshell Research Area, Southeastern Manitoba, Canada. Proceedings of Solutions '95, International Association of Hydrogeologists, Congress XXVI, June 4-10, 1995, Edmonton, Alberta, Canada.

Stevenson, D.R., A. Brown, C.C. Davison, M. Gascoyne, R.G. McGregor, D.U. Ophori, N.W. Scheier, F.W. Stanchell, G.A. Thorne and D.K. Tomsons. 1996. A revised conceptual hydrogeologic model of a crystalline rock environment, Whiteshell Research Area, southeastern Manitoba, Canada. Atomic Energy of Canada Limited Report, AECL-11331, COG-95-271.

Ticknor, K.V. and T.T. Vandergraaf. 1996. A revised compilation of sorption coefficients for use in geosphere models in performance assessments of used fuel disposal in granitic environments. Atomic Energy of Canada Limited Report, AECL-11343, COG-96-71.

TVO. 1992a. Final disposal of spent nuclear fuel in Finnish bedrock: Technical plans and safety assessment. YJT Report - 92-31E.

TVO. 1992b. Final disposal of spent nuclear fuel in the Finnish bedrock: Preliminary site investigations. YJT Report - 92-32E.

Vandergraaf, T.T., K.V. Ticknor and T.W. Melnyk. 1992. The selection and use of a sorption data base for the geosphere model in the Canadian nuclear fuel waste management program. In Radionuclide Sorption from the Safety Evaluation Perspective, proceedings of an NEA Workshop held in Interlaken, Switzerland, 1991 October, Nuclear Energy Agency, Organization for Economic Cooperation and Development, Paris, 1992.

Wikjord, A.G., P. Baumgartner, L.H. Johnson, F.W. Stanchell, R. Zach and B.W. Goodwin. 1996. The disposal of Canada's nuclear fuel waste: A study of postclosure safety of in-room emplacement of used CANDU fuel in copper containers in permeable plutonic rock. Volume 1: Summary. Atomic Energy of Canada Limited Report, AECL-11494-1, COG-95-552-1.

Zach, R., B.D. Amiro, G.A. Bird, C.R. Macdonald, M.I. Sheppard, S.C. Sheppard and J.G. Szekely. 1996. The disposal of Canada's nuclear fuel waste: A study of postclosure safety of in-room emplacement of used CANDU fuel in copper containers in permeable plutonic rock. Volume 4: Biosphere Model. Atomic Energy of Canada Limited Report, AECL-11494-4, COG-95-552-4.

TABLE 1

HYDRAULIC PROPERTY VALUES FOR THE DETAILED GROUNDWATER FLOW SIMULATIONS

Material	Permeability k_h or k_L (m^2)	Ratio of Permeabilities k_v/k_h or k_t/k_L	Porosity θ (%)
CASE 1 (EIS Case Study)			
ROCK LAYER 1	10^{-15}	5	0.5
ROCK LAYER 2	10^{-17}	5	0.4
ROCK LAYER 3	10^{-19}	1	0.3
FRACTURE ZONES	10^{-13}	0.5	10.
CASE 2			
ROCK LAYER 1	10^{-15}	5	0.5
ROCK LAYER 2	10^{-17}	5	0.4
ROCK LAYER 3	**10^{-17}**	1	**0.4**
FRACTURE ZONES	10^{-13}	0.5	10.
CASE 3			
ROCK LAYER 1	10^{-15}	5	**0.001**
ROCK LAYER 2	10^{-17}	5	**0.001**
ROCK LAYER 3	**10^{-17}**	**1**	**0.001**
FRACTURE ZONES	10^{-13}	.5	**1.**

where

k_h = Horizontal permeability (for rock layers)
k_v = Vertical permeability (for rock layers)
k_L = Longitudinal permeability (along fracture zone axis)
k_t = Transverse permeability (normal to fracture zone axis)
θ = Porosity

The BOLD text indicates a change from Case 1, the EIS Reference Case study.

TABLE 2

NODAL COORDINATES FOR GEONET

Node	x	y	z
		Units = m	
1	1027.360	-650.000	-229.400
2	475.060	-650.000	-229.400
3	352.110	-650.000	-229.400
4	106.210	-650.000	-229.400
5	-139.680	-650.000	-229.400
6	-385.580	-650.000	-229.400
7	991.094	-655.968	-286.280
8	164.756	-652.248	-42.625
9	115.726	-647.761	-42.625
10	-34.885	-653.511	-42.625
11	-210.433	-642.391	-42.625
12	-359.369	-643.072	-42.625
13	-325.151	-478.154	145.000
14	130.022	-651.359	-1.745
15	56.729	-653.096	22.477
16	-153.391	-646.004	91.920
17	-325.151	-642.920	145.000
18	1027.360	0.000	-229.400
19	475.060	0.000	-229.400
20	352.110	0.000	-229.400
21	106.210	0.000	-229.400
22	-139.680	0.000	-229.400
23	-385.580	0.000	-229.400
24	991.094	-5.968	-286.280
25	180.620	-116.740	-42.398
26	132.954	-90.153	-42.625
27	-54.307	-60.540	-42.625
28	-238.453	-32.552	-42.625
29	-413.489	-5.435	-42.625
30	-325.097	-350.000	145.000
31	150.581	-123.781	-8.380
32	79.163	-102.665	15.214
33	-175.766	-83.621	99.415
34	-323.560	-350.000	145.000
35	1027.360	650.000	-229.400
36	475.060	650.000	-229.400
37	352.110	650.000	-229.400
38	106.210	650.000	-229.400

continued...

TABLE 2 (concluded)

Node	x	y	z
		Units = m	
39	-139.680	650.000	-229.400
40	-385.580	650.000	-229.400
41	999.323	644.555	-288.164
42	144.386	310.364	-42.625
43	29.278	321.252	-42.625
44	-200.389	336.146	-42.625
45	-394.954	448.645	-42.625
46	-477.974	573.722	-42.625
47	-325.050	-222.659	145.000
48	85.774	279.947	13.136
49	-167.900	225.726	96.873
50	-323.560	124.049	145.000
51	-631.480	-650.000	-229.400
52	-631.480	0.000	-229.400
53	-631.480	650.000	-229.400
54	-1005.330	-950.000	-229.400
55	-1005.330	0.000	-229.400
56	-1005.330	950.000	-229.400
57	-609.672	-552.066	-42.625
58	-621.178	5.177	-42.625
59	-649.082	573.261	-42.625
60	-1277.600	-907.320	-227.600
61	-1028.222	26.231	-42.625
62	-1092.733	821.237	-42.625
63	-607.610	-517.820	37.779
64	-627.635	8.107	42.947
65	-660.090	543.720	53.029
66	-1193.063	736.381	148.710
67	-899.799	49.103	148.710
68	-1294.444	-842.665	148.710
69	-911.395	50.828	255.000
70	-1295.800	660.680	255.000
71	-1325.800	-834.720	255.000
72	-424.812	-350.000	185.475
73	-424.812	-350.000	255.000
74	-526.063	-350.000	217.191
75	-534.590	-350.000	219.862
76	-536.721	-350.000	220.529
77	-536.721	-350.000	255.000

TABLE 3

GEONET SEGMENT, PHYSICAL & CHEMICAL PROPERTY CLASSES

Segment	Physical Class	Chemical Class	Inlet Node	Outlet Node
1	1	1	1	7
2	1	1	2	8
3	1	1	3	9
4	1	1	4	10
5	1	1	5	11
6	1	1	6	12
7	2	2	8	14
8	2	2	9	15
9	2	2	10	16
10	2	2	11	17
11	2	2	12	17
12	4	4	7	13
13	4	4	14	17
14	4	4	15	17
15	4	4	16	17
16	1	1	18	24
17	1	1	19	25
18	1	1	20	26
19	1	1	21	27
20	1	1	22	28
21	1	1	23	29
22	2	2	25	31
23	2	2	26	32
24	2	2	27	33
25	2	2	28	34
26	2	2	29	34
27	4	4	24	30
28	4	4	31	34
29	4	4	32	34
30	4	4	33	34
31	1	1	35	41
32	1	1	36	42
33	1	1	37	43
34	1	1	38	44
35	1	1	39	45
36	1	1	40	46
37	2	2	42	48
38	2	2	43	49
39	2	2	44	50
40	2	2	45	50

continued...

TABLE 3 (concluded)

Segment	Physical Class	Chemical Class	Inlet Node	Outlet Node
41	2	2	46	50
42	4	4	41	47
43	4	4	48	50
44	4	4	49	50
45	1	1	51	57
46	1	1	52	58
47	1	1	53	59
48	1	1	54	60
49	1	1	55	61
50	1	1	56	62
51	2	2	57	63
52	2	2	58	64
53	2	2	59	65
54	4	4	60	68
55	2	2	61	67
56	2	2	62	66
57	4	4	63	67
58	4	4	64	67
59	4	4	65	67
60	3	3	66	70
61	3	3	67	69
62	4	4	68	71
63	10	10	34	17
64	10	10	34	50
65	10	10	30	13
66	10	10	30	47
67	10	10	17	72
68	10	10	50	72
69	10	10	13	72
70	10	10	47	72
71	3	3	72	73
72	4	4	34	74
73	4	4	30	74
74	4	4	74	75
75	4	4	75	76
76	10	10	76	77
77	4	4	17	74
78	4	4	50	74
79	4	4	13	74
80	4	4	47	74

TABLE 4

GEONET SEGMENT PERMEABILITIES

Segment	Physical Class	Permeability m^2
1	1	0.10000E-16
2	1	0.10000E-16
3	1	0.10000E-16
4	1	0.10000E-16
5	1	0.10000E-16
6	1	0.10000E-16
7	2	0.33224E-16
8	2	0.31882E-16
9	2	0.32486E-16
10	2	0.39115E-16
11	2	0.46504E-16
12	4	0.87053E-13
13	4	0.87481E-13
14	4	0.87524E-13
15	4	0.88029E-13
16	1	0.10000E-16
17	1	0.10000E-16
18	1	0.10000E-16
19	1	0.10000E-16
20	1	0.10000E-16
21	1	0.10000E-16
22	2	0.31947E-16
23	2	0.30924E-16
24	2	0.32758E-16
25	2	0.19832E-16
26	2	0.18691E-16
27	4	0.88410E-13
28	4	0.89771E-13
29	4	0.90575E-13
30	4	0.94291E-13
31	1	0.10000E-16
32	1	0.10000E-16
33	1	0.10000E-16
34	1	0.10000E-16
35	1	0.10000E-16
36	1	0.10000E-16
37	2	0.26650E-16
38	2	0.21538E-16
39	2	0.24767E-16
40	2	0.19667E-16

continued...

TABLE 4 (concluded)

Segment	Physical Class	Permeability m^2
41	2	0.15390E-16
42	4	0.90654E-13
43	4	0.89270E-13
44	4	0.91161E-13
45	1	0.10000E-16
46	1	0.10000E-16
47	1	0.10000E-16
48	1	0.10000E-16
49	1	0.10000E-16
50	1	0.10000E-16
51	2	0.43839E-16
52	2	0.49200E-16
53	2	0.46081E-16
54	4	0.53362E-13
55	2	0.37308E-16
56	2	0.37180E-16
57	4	0.90815E-13
58	4	0.84556E-13
59	4	0.93841E-13
60	3	0.26383E-14
61	3	0.48613E-14
62	4	0.53272E-13
63	10	0.00000E+00
64	10	0.00000E+00
65	10	0.00000E+00
66	10	0.00000E+00
67	10	0.00000E+00
68	10	0.00000E+00
69	10	0.00000E+00
70	10	0.00000E+00
71	3	0.21139E-14
72	4	0.86135E-13
73	4	0.86024E-13
74	4	0.87904E-13
75	4	0.87914E-13
76	10	0.00000E+00
77	4	0.89912E-13
78	4	0.94431E-13
79	4	0.86768E-13
80	4	0.89579E-13

TABLE 5

POROSITY OF THE ROCK ZONES FOR GEONET

Physical Property Zone	Physical Class	Distribution Type	Value Minimum	Value Maximum
lower rock zone	1	Uniform	0.00001	0.001
middle rock zone	2	Uniform	0.00001	0.001
upper rock zone	3	Uniform	0.00001	0.001
fracture zone LD1	4	Uniform	0.10000	0.010

TABLE 6

GEONET SEGMENT DISPERSIVITIES

Segment	Physical Class	Dispersivity Ratio Minimum	Maximum
1	1	0.01	0.9
2	1	0.01	0.9
3	1	0.01	0.9
4	1	0.01	0.9
5	1	0.01	0.9
6	1	0.01	0.9
7	2	0.01	0.9
8	2	0.01	0.9
9	2	0.01	0.9
10	2	0.01	0.9
11	2	0.01	0.9
12	4	0.01	0.25
13	4	0.01	0.25
14	4	0.01	0.25
15	4	0.01	0.25
16	1	0.01	0.9
17	1	0.01	0.9
18	1	0.01	0.9
19	1	0.01	0.9
20	1	0.01	0.9
21	1	0.01	0.9
22	2	0.01	0.9
23	2	0.01	0.9
24	2	0.01	0.9
25	2	0.01	0.9
26	2	0.01	0.9
27	4	0.01	0.25
28	4	0.01	0.25
29	4	0.01	0.25
30	4	0.01	0.25
31	1	0.01	0.9
32	1	0.01	0.9
33	1	0.01	0.9
34	1	0.01	0.9
35	1	0.01	0.9
36	1	0.01	0.9
37	2	0.01	0.9
38	2	0.01	0.9
39	2	0.01	0.9
40	2	0.01	0.9

continued...

TABLE 6 (concluded)

Segment	Physical Class	Dispersivity Ratio	
		Minimum	Maximum
41	2	0.01	0.9
42	4	0.01	0.25
43	4	0.01	0.25
44	4	0.01	0.25
45	1	0.01	0.9
46	1	0.01	0.9
47	1	0.01	0.9
48	1	0.01	0.9
49	1	0.01	0.9
50	1	0.01	0.9
51	2	0.01	0.9
52	2	0.01	0.9
53	2	0.01	0.9
54	4	0.01	0.25
55	2	0.01	0.9
56	2	0.01	0.9
57	4	0.01	0.25
58	4	0.01	0.25
59	4	0.01	0.25
60	3	0.01	0.9
61	3	0.01	0.9
62	4	0.01	0.25
63	10	0.00	0.0
64	10	0.00	0.0
65	10	0.00	0.0
66	10	0.00	0.0
67	10	0.00	0.0
68	10	0.00	0.0
69	10	0.00	0.0
70	10	0.00	0.0
71	3	0.01	0.9
72	4	0.01	0.25
73	4	0.01	0.25
74	4	0.01	0.25
75	4	0.01	0.25
76	10	0.00	0.0
77	4	0.01	0.25
78	4	0.01	0.25
79	4	0.01	0.25
80	4	0.01	0.25

TABLE 7

GEONET HYDRAULIC HEADS

Node	Value m
1	0.2674957E+03
2	0.2634654E+03
3	0.2627983E+03
4	0.2614354E+03
5	0.2601681E+03
6	0.2595315E+03
7	0.2662704E+03
8	0.2612136E+03
9	0.2608288E+03
10	0.2596079E+03
11	0.2581985E+03
12	0.2578316E+03
13	0.2565398E+03
14	0.2608569E+03
15	0.2602636E+03
16	0.2581255E+03
17	0.2564772E+03
18	0.2688524E+03
19	0.2642543E+03
20	0.2635523E+03
21	0.2620448E+03
22	0.2604521E+03
23	0.2591587E+03
24	0.2670738E+03
25	0.2620366E+03
26	0.2616889E+03
27	0.2600844E+03
28	0.2583580E+03
29	0.2572666E+03
30	0.2566028E+03
31	0.2617241E+03
32	0.2611660E+03
33	0.2584950E+03
34	0.2566151E+03
35	0.2697218E+03
36	0.2663111E+03
37	0.2657945E+03

continued...

TABLE 7 (concluded)

Node	Value m
38	0.2646715E+03
39	0.2632875E+03
40	0.2614742E+03
41	0.2684383E+03
42	0.2631822E+03
43	0.2623618E+03
44	0.2602419E+03
45	0.2586501E+03
46	0.2583090E+03
47	0.2567367E+03
48	0.2625936E+03
49	0.2597479E+03
50	0.2574028E+03
51	0.2594169E+03
52	0.2585153E+03
53	0.2601426E+03
54	0.2594014E+03
55	0.2581629E+03
56	0.2604625E+03
57	0.2587050E+03
58	0.2571964E+03
59	0.2582841E+03
60	0.2579019E+03
61	0.2569501E+03
62	0.2582803E+03
63	0.2584827E+03
64	0.2570002E+03
65	0.2578826E+03
66	0.2569832E+03
67	0.2563746E+03
68	0.2565297E+03
69	0.2550000E+03
70	0.2550000E+03
71	0.2550000E+03
72	0.2557939E+03
73	0.2550000E+03
74	0.2553021E+03
75	0.2552623E+03
76	0.2552524E+03
77	0.2550000E+03

TABLE 8

GEONET NODAL TEMPERATURES

Node	Value °C
1	0.1993914E+02
2	0.2844187E+02
3	0.3074545E+02
4	0.3267625E+02
5	0.3332054E+02
6	0.3282236E+02
7	0.1990765E+02
8	0.2197858E+02
9	0.2223569E+02
10	0.2250415E+02
11	0.2261881E+02
12	0.2231236E+02
13	0.1272754E+02
14	0.1994158E+02
15	0.1884697E+02
16	0.1524153E+02
17	0.1214797E+02
18	0.2136471E+02
19	0.3151944E+02
20	0.3427144E+02
21	0.3684910E+02
22	0.3775986E+02
23	0.3713310E+02
24	0.2140127E+02
25	0.2468987E+02
26	0.2503199E+02
27	0.2572878E+02
28	0.2571648E+02
29	0.2517511E+02
30	0.1315512E+02
31	0.2277582E+02
32	0.2170168E+02
33	0.1667051E+02
34	0.1315983E+02
35	0.1986846E+02
36	0.2828135E+02
37	0.3058674E+02
38	0.3255886E+02

continued...

TABLE 8 (Continued)

Node	Value °C
39	0.3326235E+02
40	0.3281748E+02
41	0.1988267E+02
42	0.2441815E+02
43	0.2488826E+02
44	0.2507498E+02
45	0.2378461E+02
46	0.2243769E+02
47	0.1331569E+02
48	0.2138920E+02
49	0.1662866E+02
50	0.1348787E+02
51	0.3119844E+02
52	0.3501329E+02
53	0.3121970E+02
54	0.1885411E+02
55	0.2557784E+02
56	0.1884930E+02
57	0.2177791E+02
58	0.2380341E+02
59	0.2138297E+02
60	0.1474684E+02
61	0.1778218E+02
62	0.1397216E+02
63	0.1760365E+02
64	0.1868299E+02
65	0.1645126E+02
66	0.8803936E+01
67	0.1113605E+02
68	0.8234212E+01
69	0.6000000E+01
70	0.6000000E+01
71	0.6000000E+01
72	0.1044509E+02
73	0.6000000E+01
74	0.8337121E+01
75	0.8159811E+01
76	0.8115531E+01
77	0.6000000E+01

TABLE 9

GEONET DISCHARGE AREA PARAMETERS

Parameter Name	Distribution Type	Value	Units
Discharge area			
Boggy Creek North	constant	5.9×10^4	m^2
Boggy Creek South	constant	2.24×10^5	m^2
Pinawa Channel North	constant	7.0×10^4	m^2
Pinawa Channel South	constant	1.12×10^5	m^2

TABLE 10

NODE SPECIFIC CONSTANTS FOR THE EMPIRICAL EQUATIONS FOR CALCULATING HYDRAULIC HEAD CHANGE DUE TO A WELL

Node	A_o
2	-0.4385703E-04
3	-0.4817527E-04
4	-0.5782427E-04
5	-0.6301444E-04
6	-0.4216439E-04
8	-0.6922150E-04
9	-0.7319641E-04
10	-0.7958221E-04
11	-0.7724217E-04
12	-0.4578182E-04
19	-0.4374695E-04
20	-0.4745047E-04
21	-0.5416107E-04
22	-0.5354200E-04
23	-0.3420367E-04
25	-0.7379914E-04
26	-0.7681057E-04
27	-0.8567592E-04
28	-0.6850760E-04
29	-0.1217869E-04
36	-0.2365657E-04
37	-0.2330998E-04
38	-0.2022879E-04
39	-0.1452201E-04
40	-0.8282253E-05
42	-0.3988211E-04
43	-0.3641728E-04
44	-0.2022879E-04
45	-0.3559657E-05
46	-0.4675729E-06

TABLE 11

PARTITIONING OF GEOSPHERE PATHWAYS AT WELL CAPTURE NODES

		Width (metres)
Pathways from RHS, above LD1		
	segment 73	128
	segment 79	128
	segment 80	127
Pathways from LHS, below LD1		
	segment 72	292
	segment 77	294
	segment 78	656
Pathways width at capture line		1242

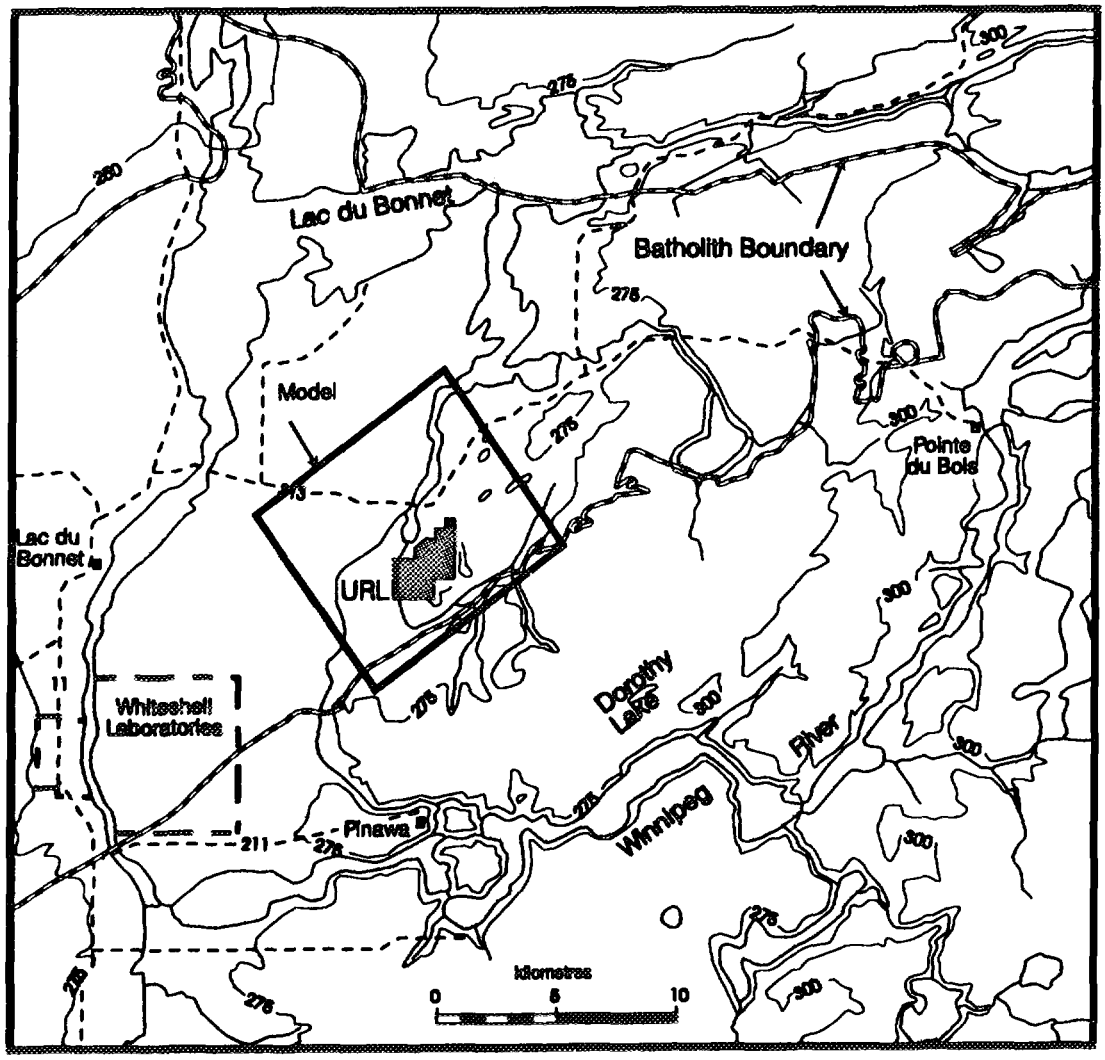

FIGURE 1: The Geographic Location of the Geosphere Model

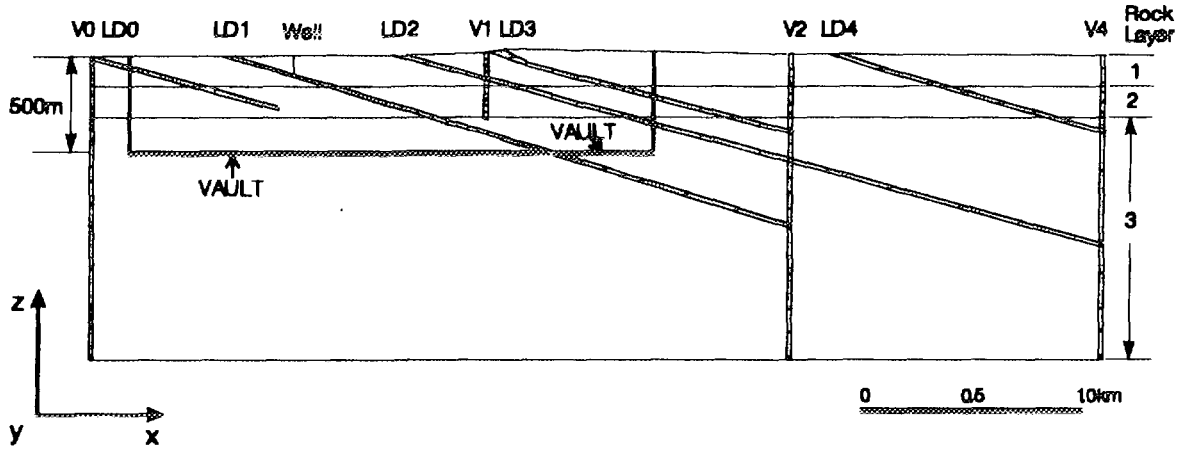

FIGURE 2: Vertical Section of the Geometry of the Hypothetical Geosphere Model

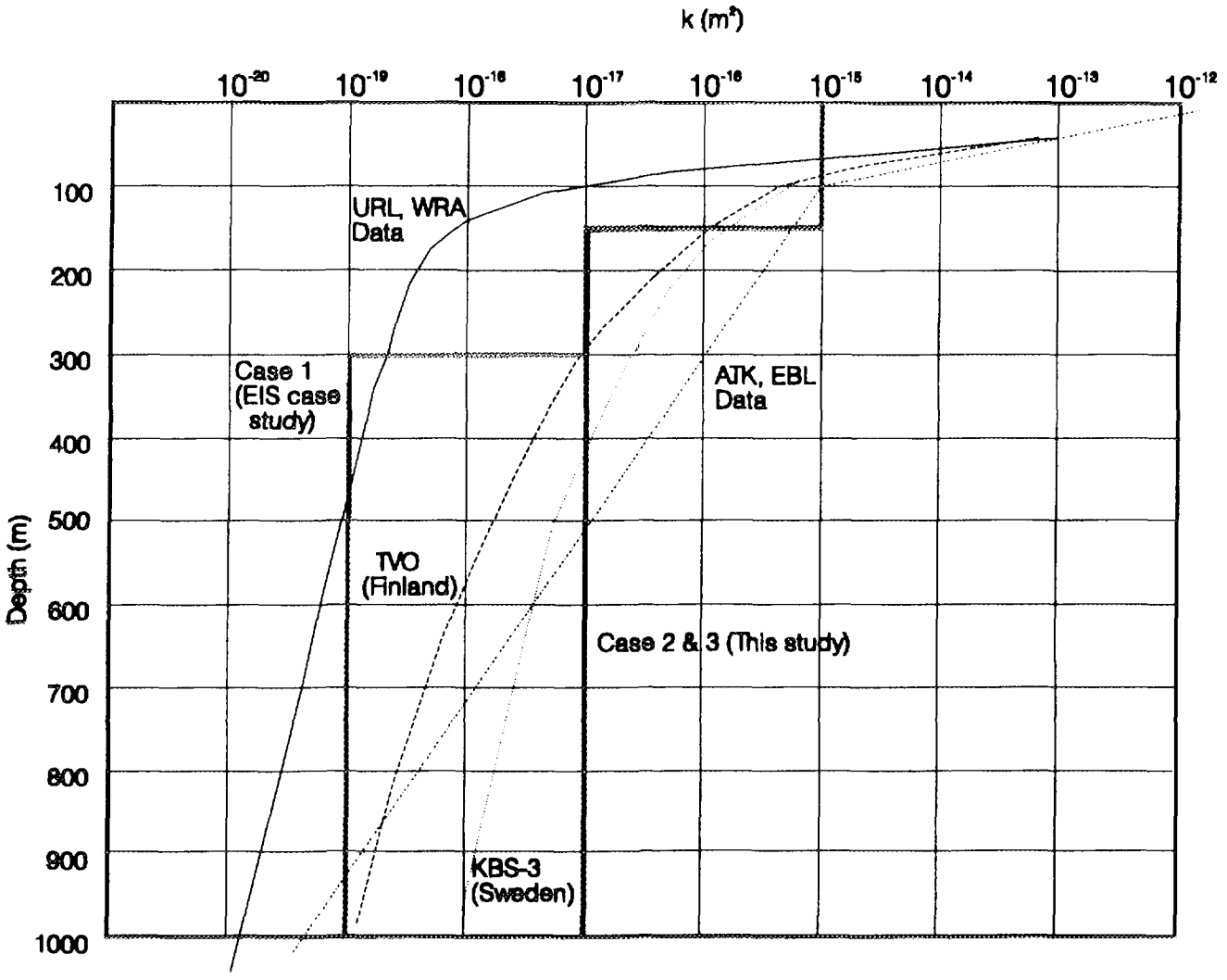

FIGURE 3: Permeability Versus Depth Data for Rocks at AECL's Research Areas, Swedish and Finnish Assessments of Fennoscandian Shield Conditions and Conditions Assumed in this Study

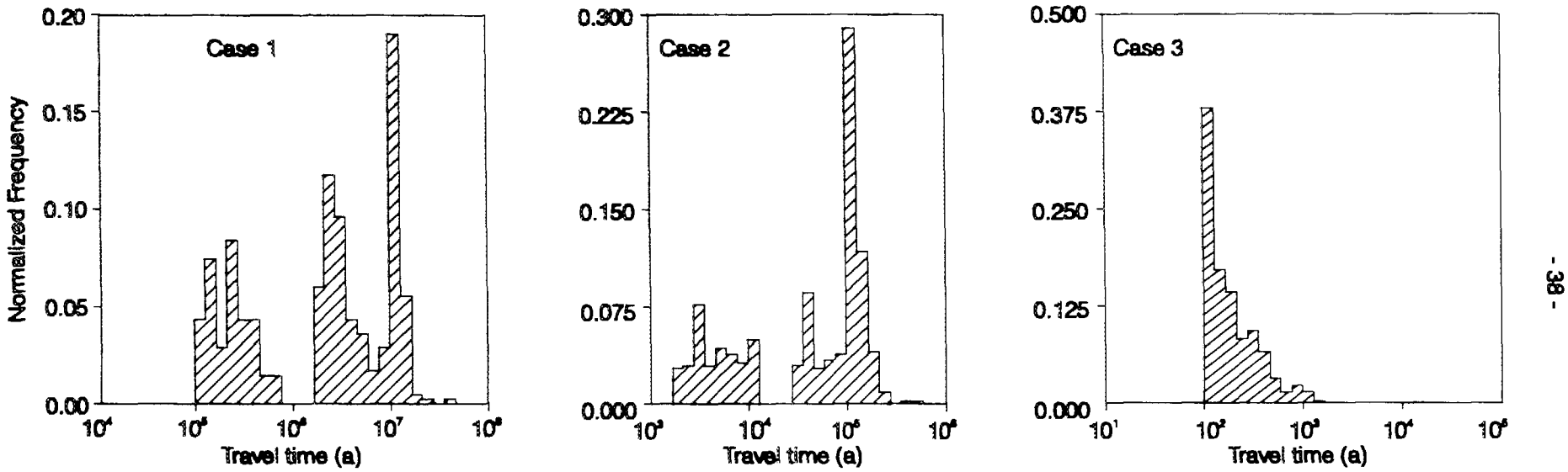

FIGURE 4: Advective Particle Travel Times from the Vault to the Ground Surface for the Three Isothermal Cases

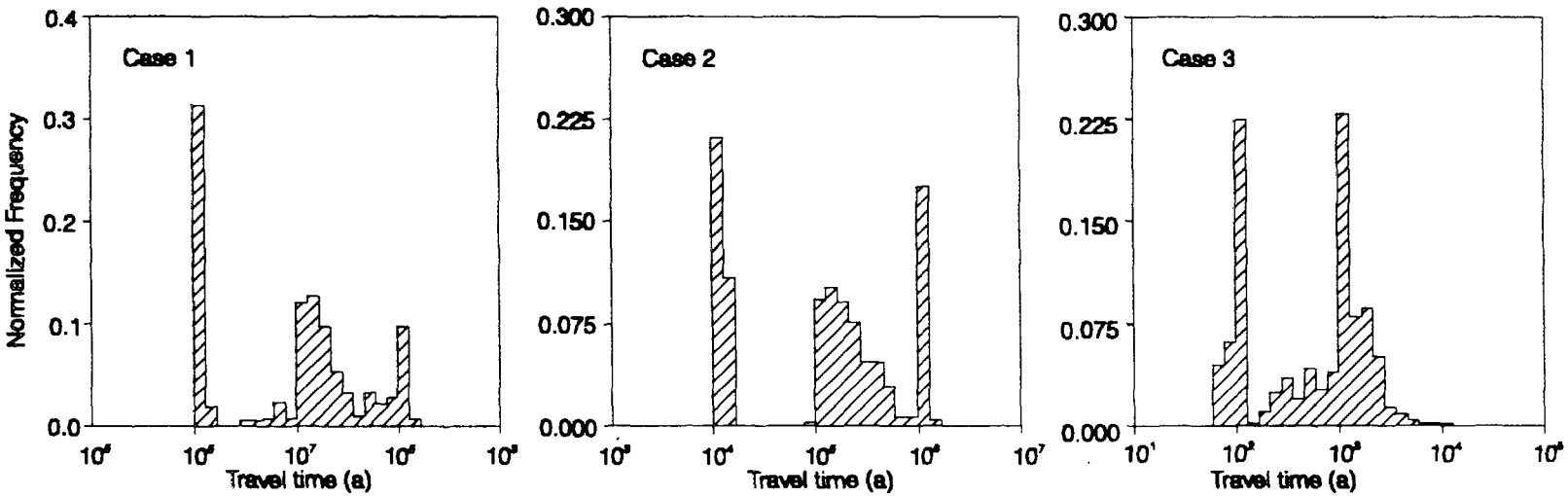

FIGURE 5: Calculated Groundwater Age at Disposal Vault Depth for the Three Isothermal Cases

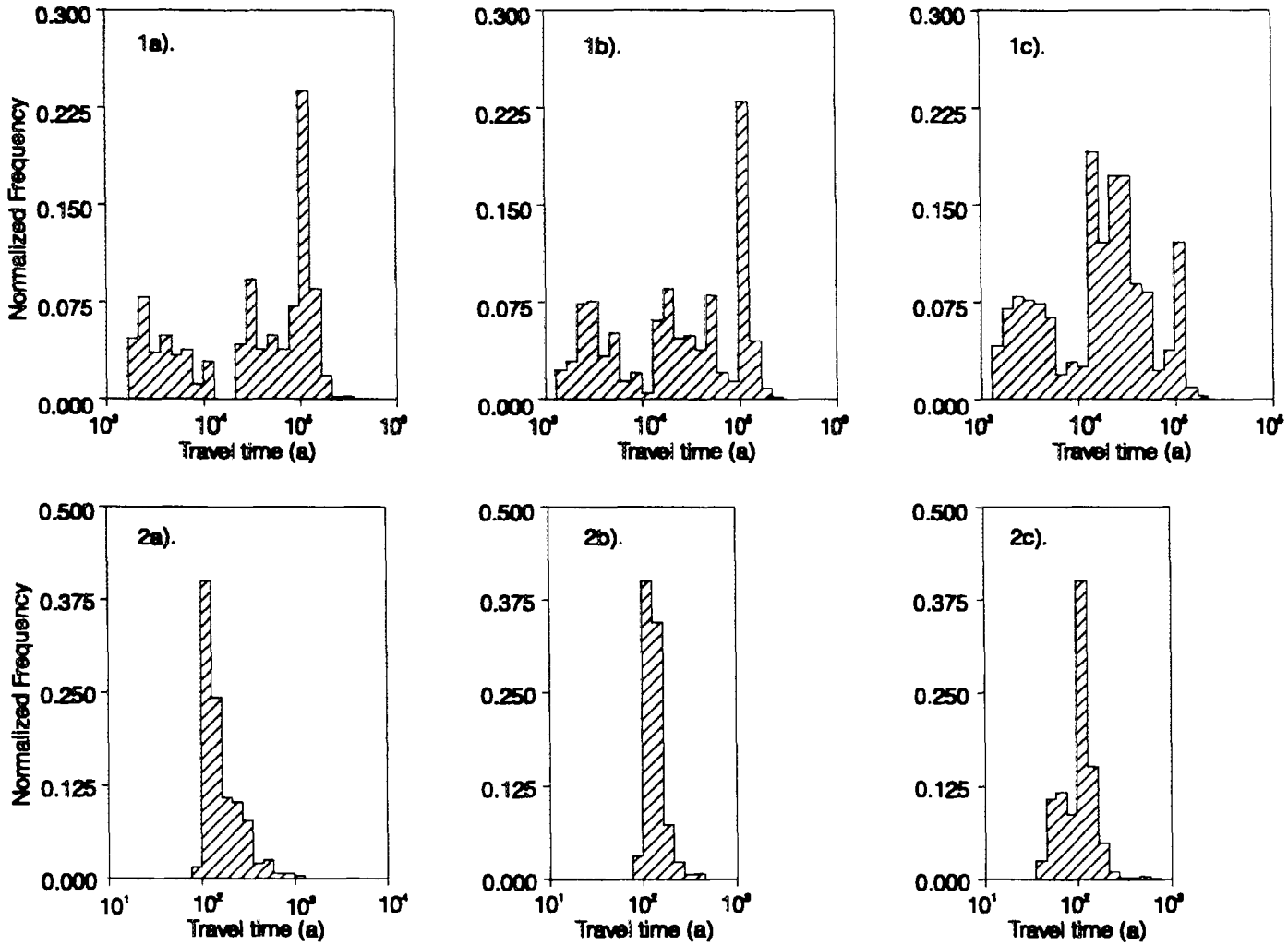

FIGURE 6: Advective Particle Travel Times to the Ground Surface for Starting Locations in the Vault
(1). Case 2 a). Geothermal Gradient, b). Geothermal Gradient and Waste Heat, and c). Geothermal Gradient and Waste Heat Maximum Velocity Field
(2). Case 3 a). Geothermal Gradient, b). Geothermal Gradinet and Waste Heat, and c). Geothermal Gradient and Waste Heat Maximum Velocity Field

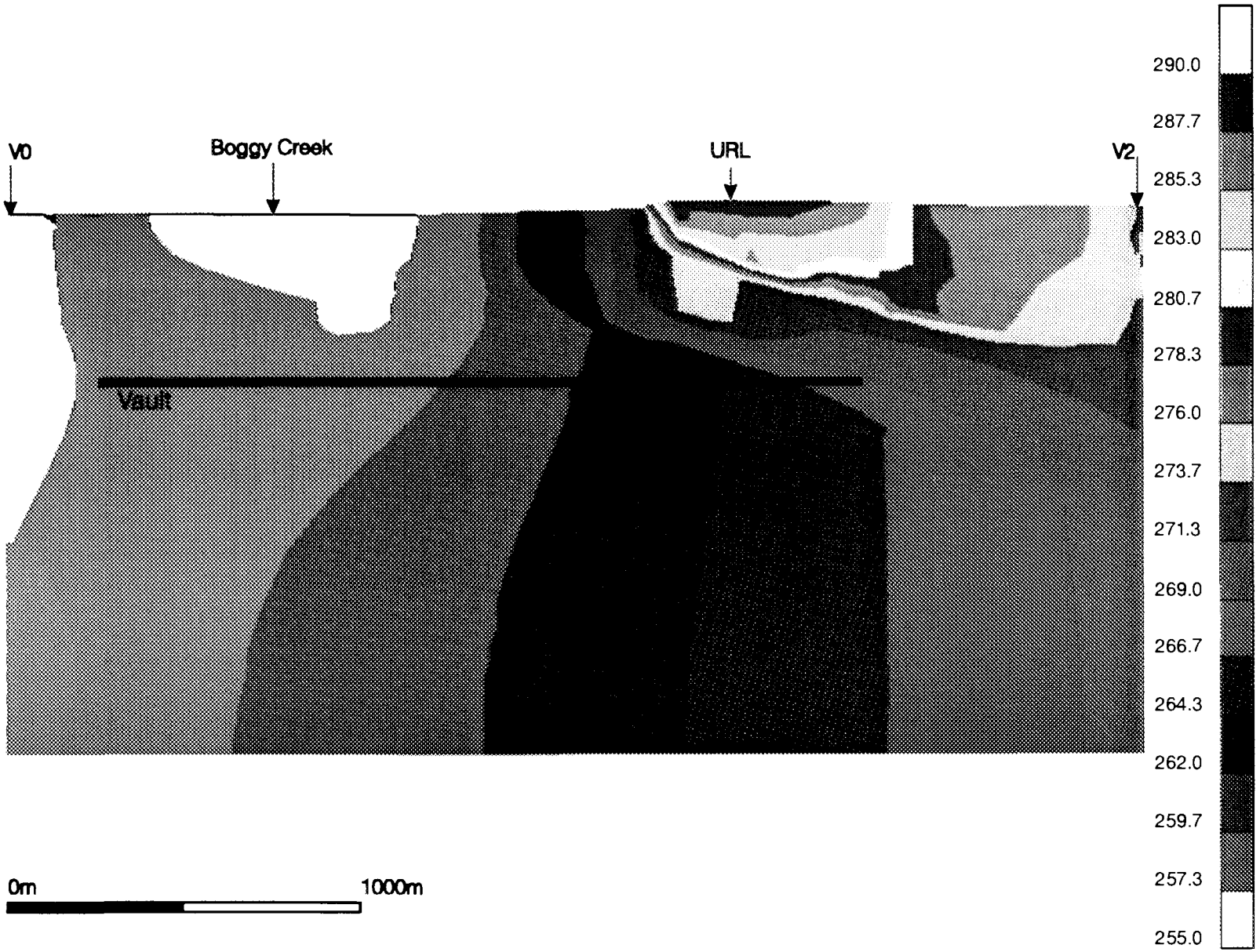

FIGURE 7: Head Distribution in the Vicinity of the Vault for the Isothermal Case 1

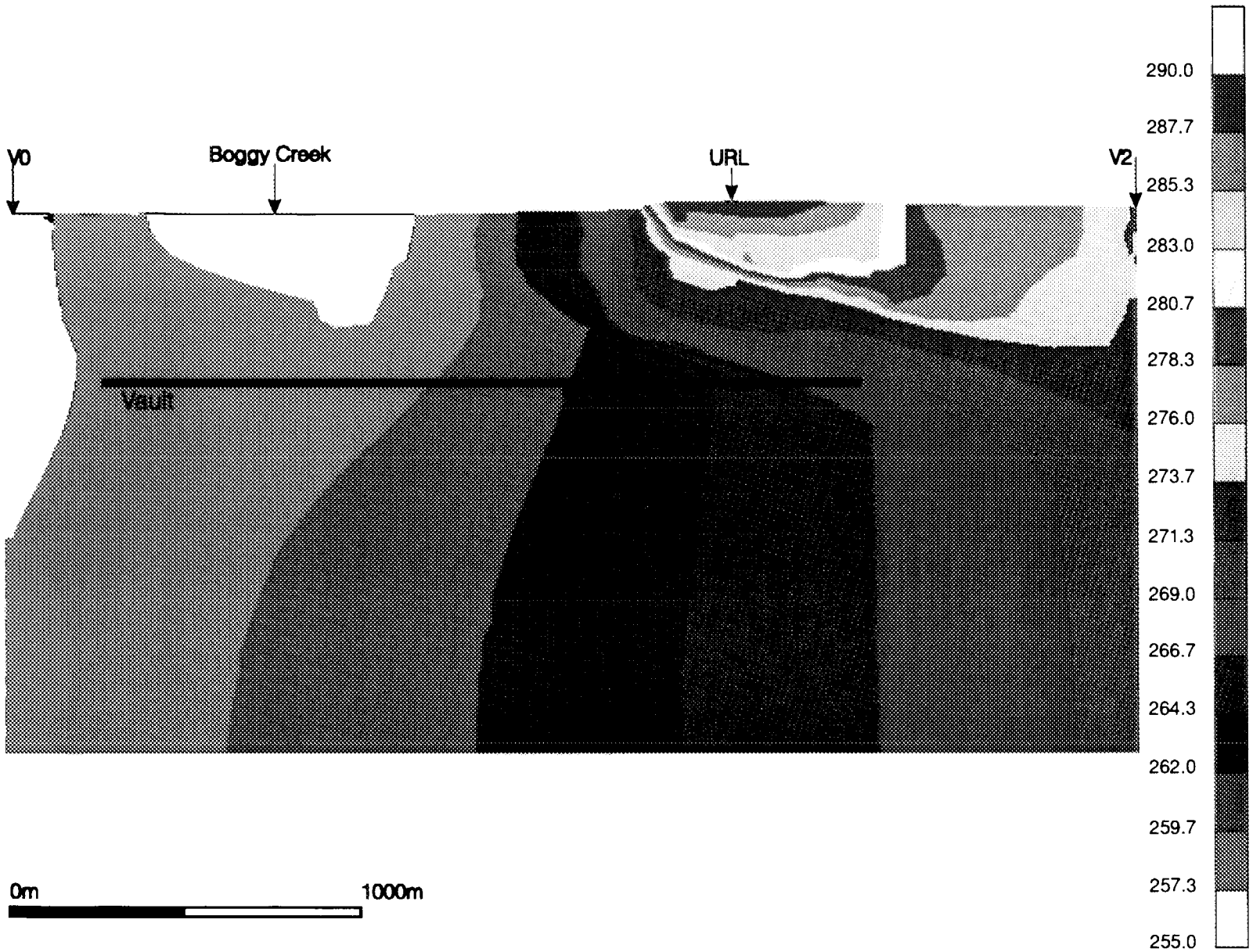

FIGURE 8: Head Distribution in the Vicinity of the Vault for the Isothermal Case 2

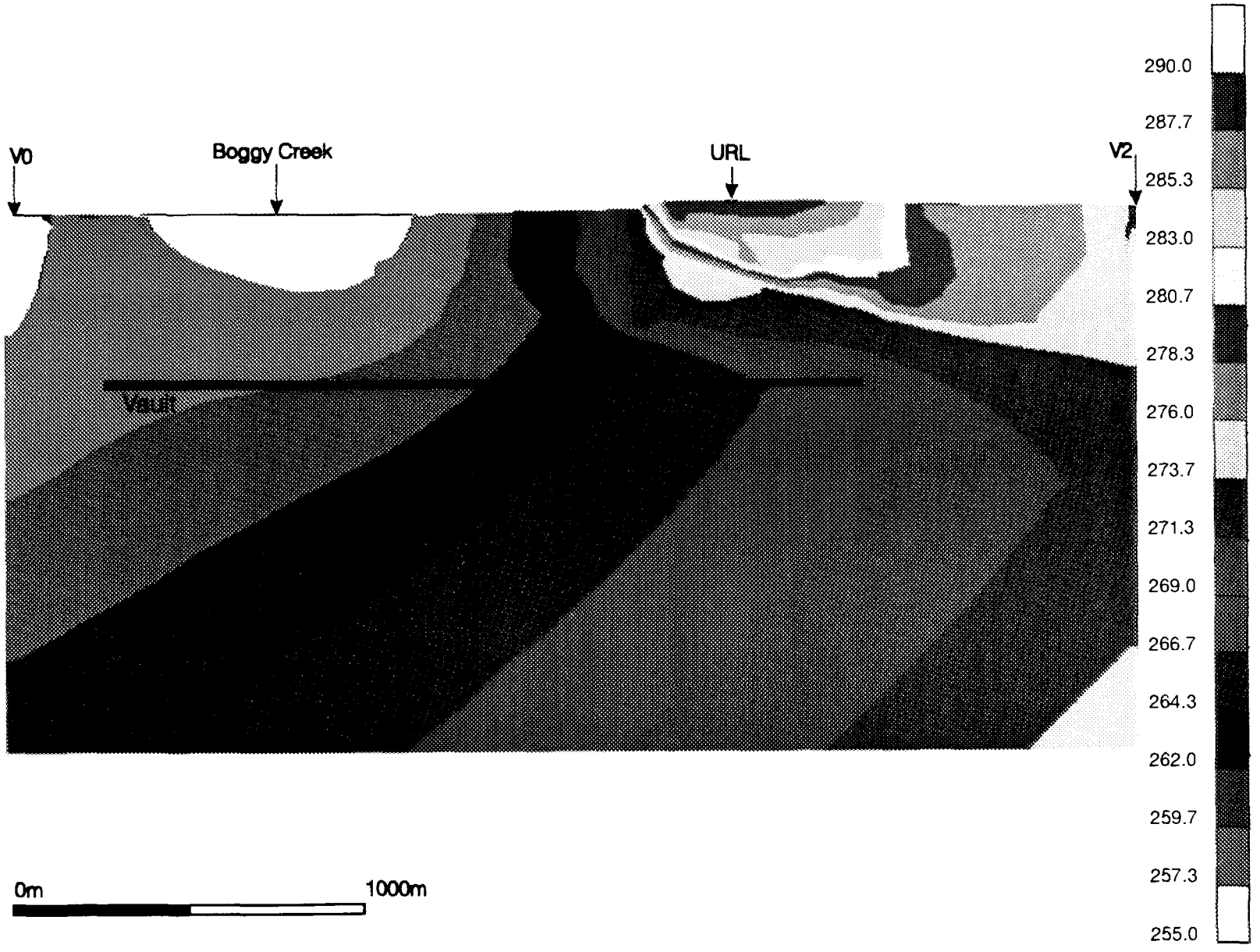

FIGURE 9: Head Distribution in the Vicinity of the Vault for Case 2 Including the Geothermal Gradient

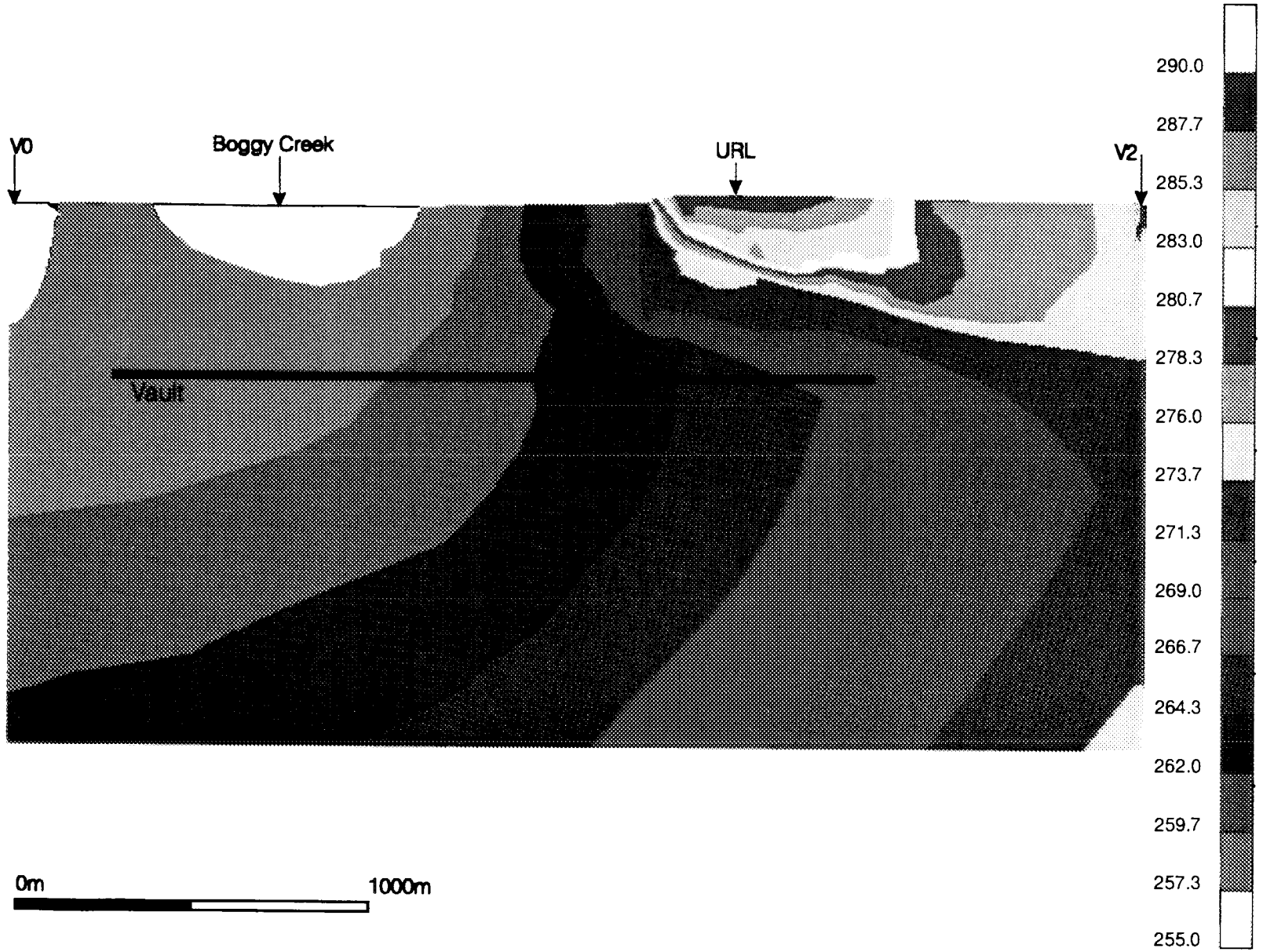

Figure 10: Head Distribution in the Vicinity of the Vault for Case 2 Including the Geothermal Gradient and Waste Heat

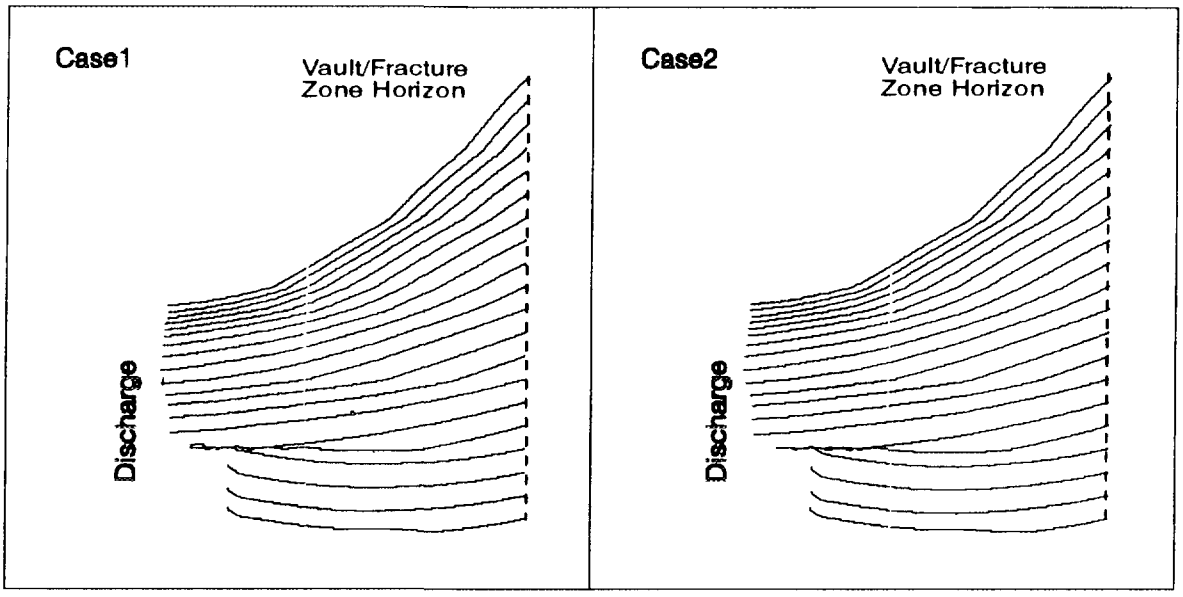

FIGURE 11: Particle Tracks Illustrating the Flow Field in Fracture Zone LD1 for the Isothermal Case 1 and Case 2

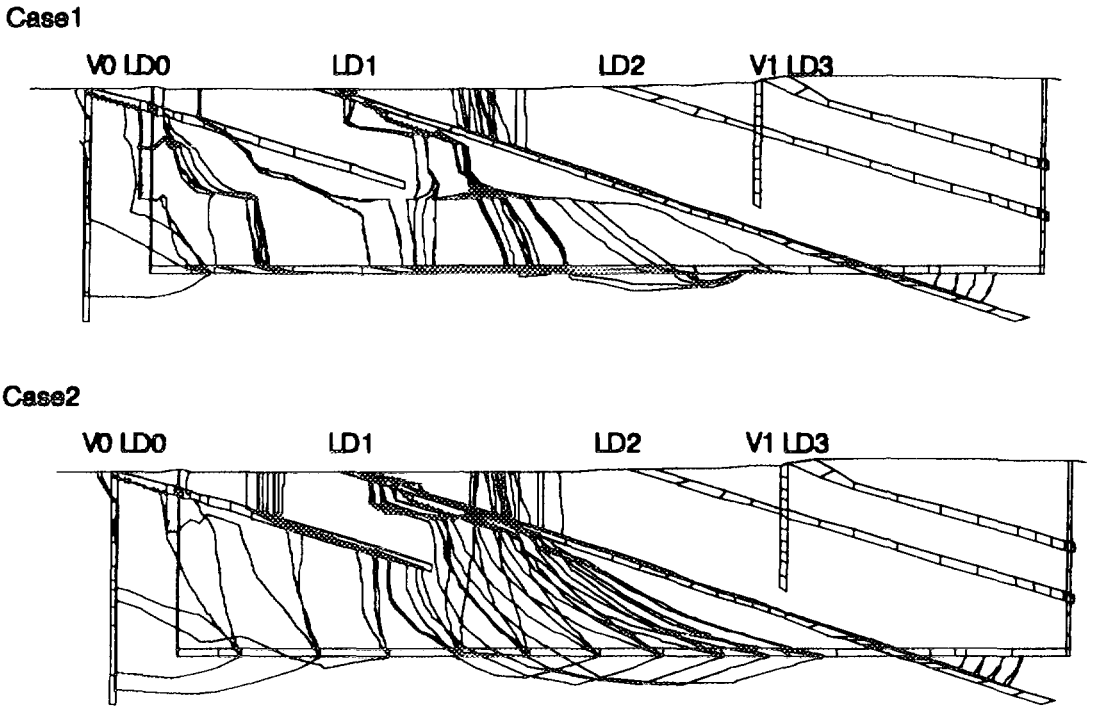

FIGURE 12: Particle Tracks Illustrating Groundwater Flow Pathways from the Vault for the Isothermal Case 1 and Case 2

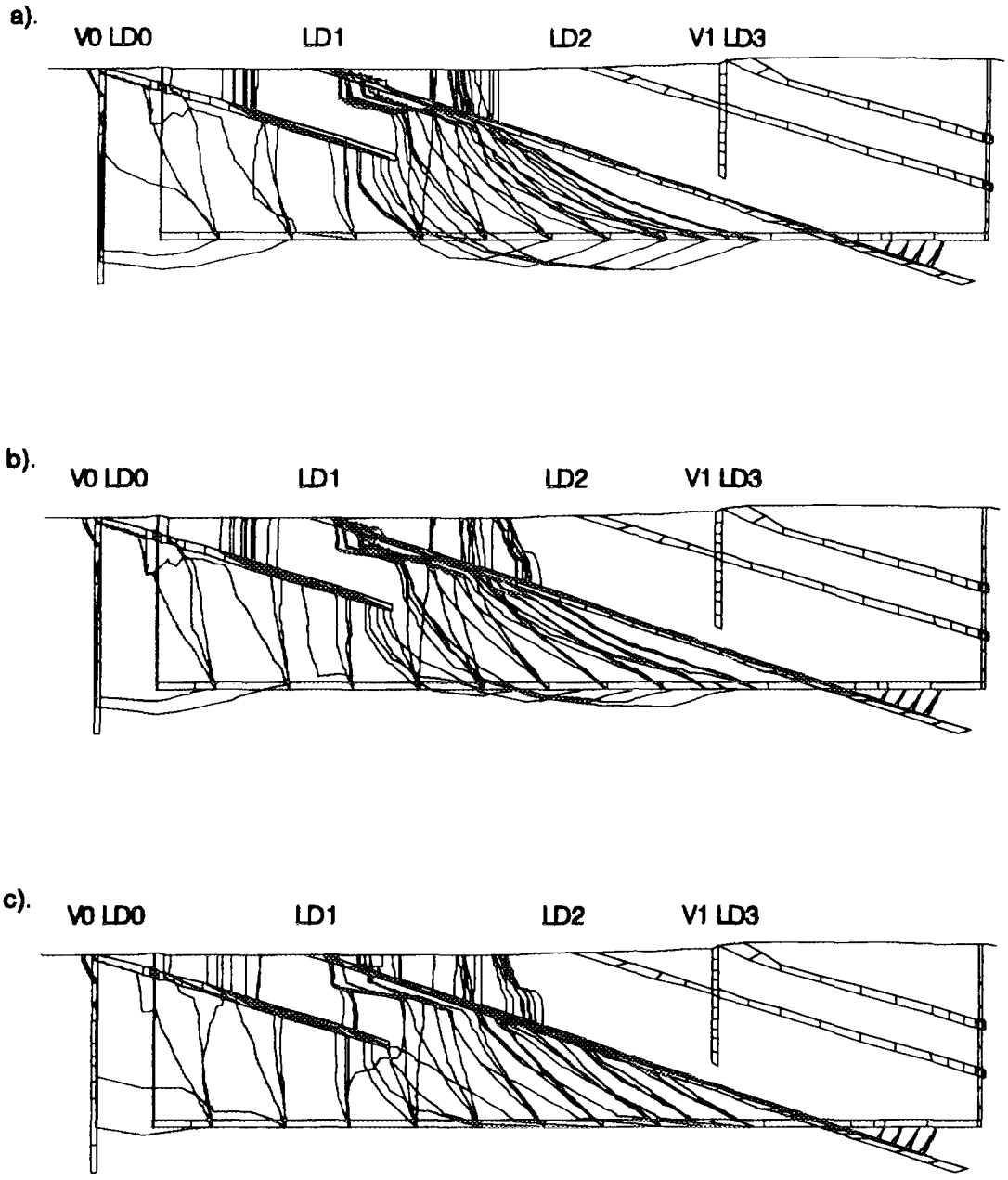

FIGURE 13: Particle Tracks Illustrating Groundwater Flow Pathways from the Vault for Case 2
a). Including the Geothermal Gradient,
b). Including the Geothermal Gradient and Waste Heat, and
c). Including the Geothermal Gradient and Waste Heat Maximum Velocity Field

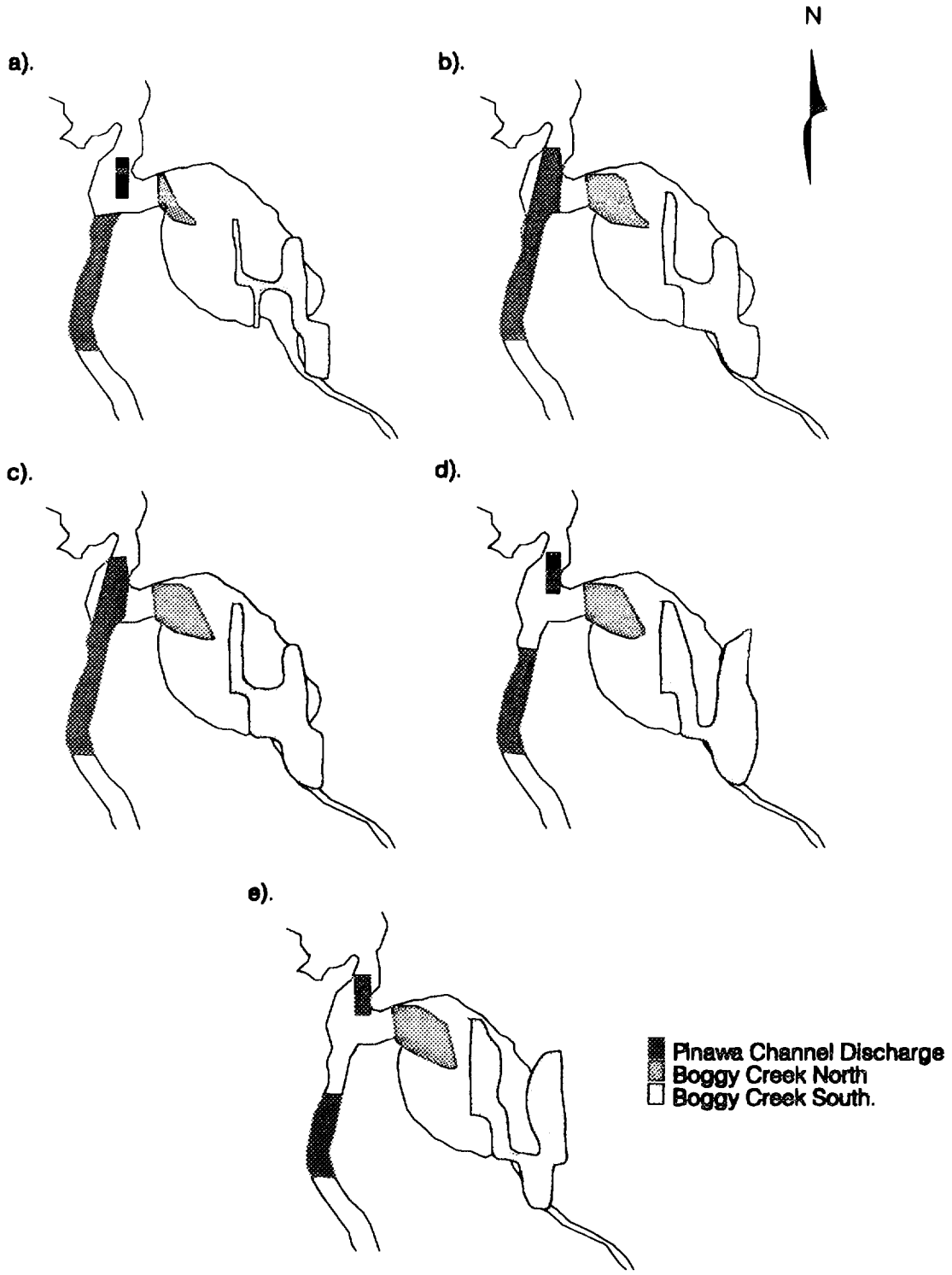

FIGURE 14: The Surface Discharge Locations of Groundwater Pathways Starting at the Vault for
a). Isothermal Case 1,
b). Isothermal Case 2,
c). Geothermal Gradient Case 2,
d). Geothermal Gradient Plus Waste Heat Case 2, and
e). Geothermal Gradient Plus Waste Heat Maximum Velocity Field Case 2

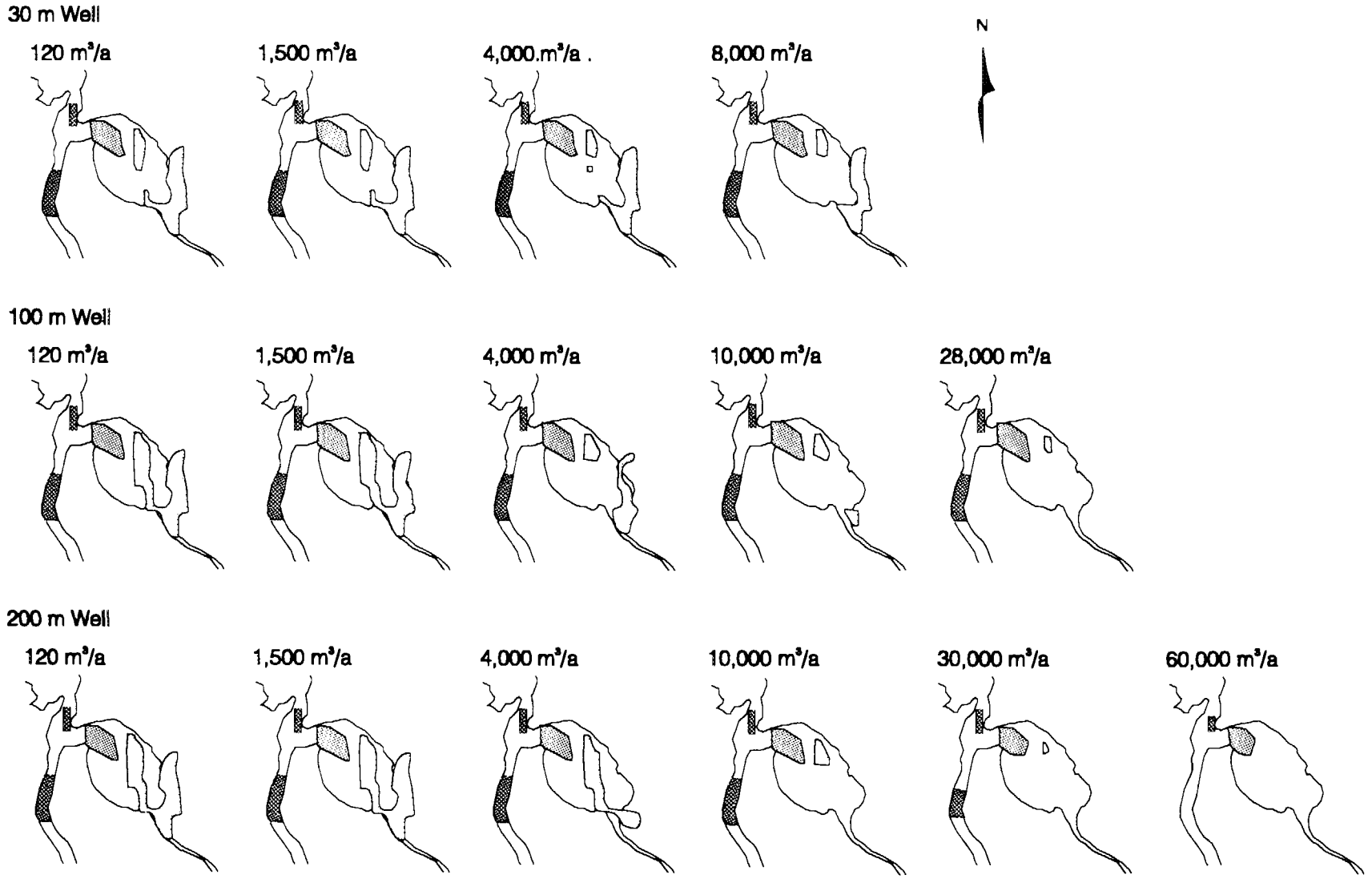

FIGURE 15: The Surface Discharge Areas of Groundwater Pathways from the Vault for 3 Different Well Depths and Various Well Demands up to the Well Capacity for Case 2 with Geothermal Gradient Plus Waste Heat, Maximum Velocity Field.

a).

b).

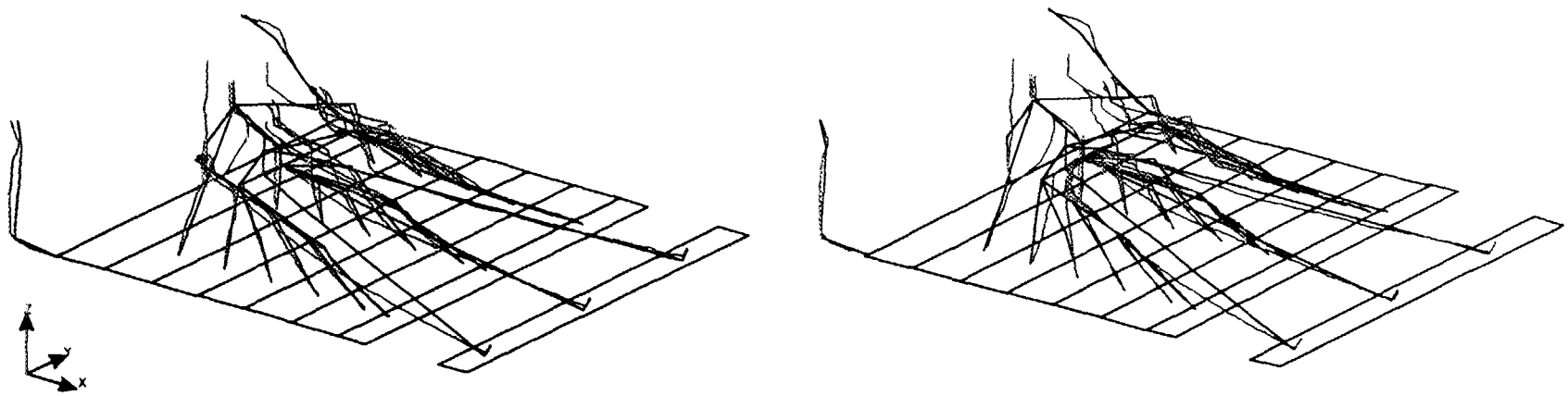

Particle flow path

FIGURE 16: Preliminary GEONET Network of Groundwater Pathways from the Vault Sectors (Superimposed on Particle Tracks) for a). the No Well Case and b). Case with a 10,000 m^3/a 100m Deep Well.

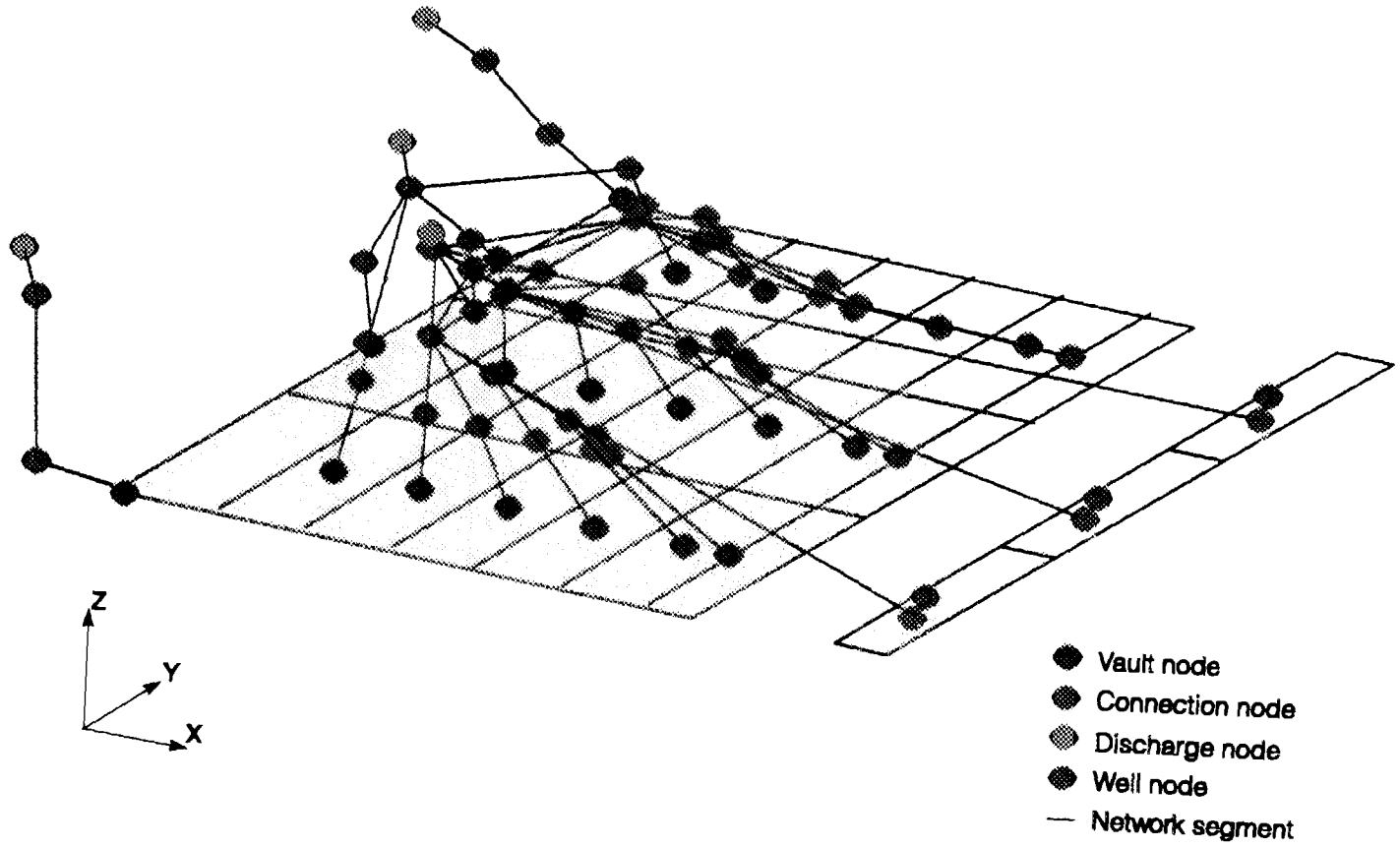

FIGURE 17: The Final GEONET Network

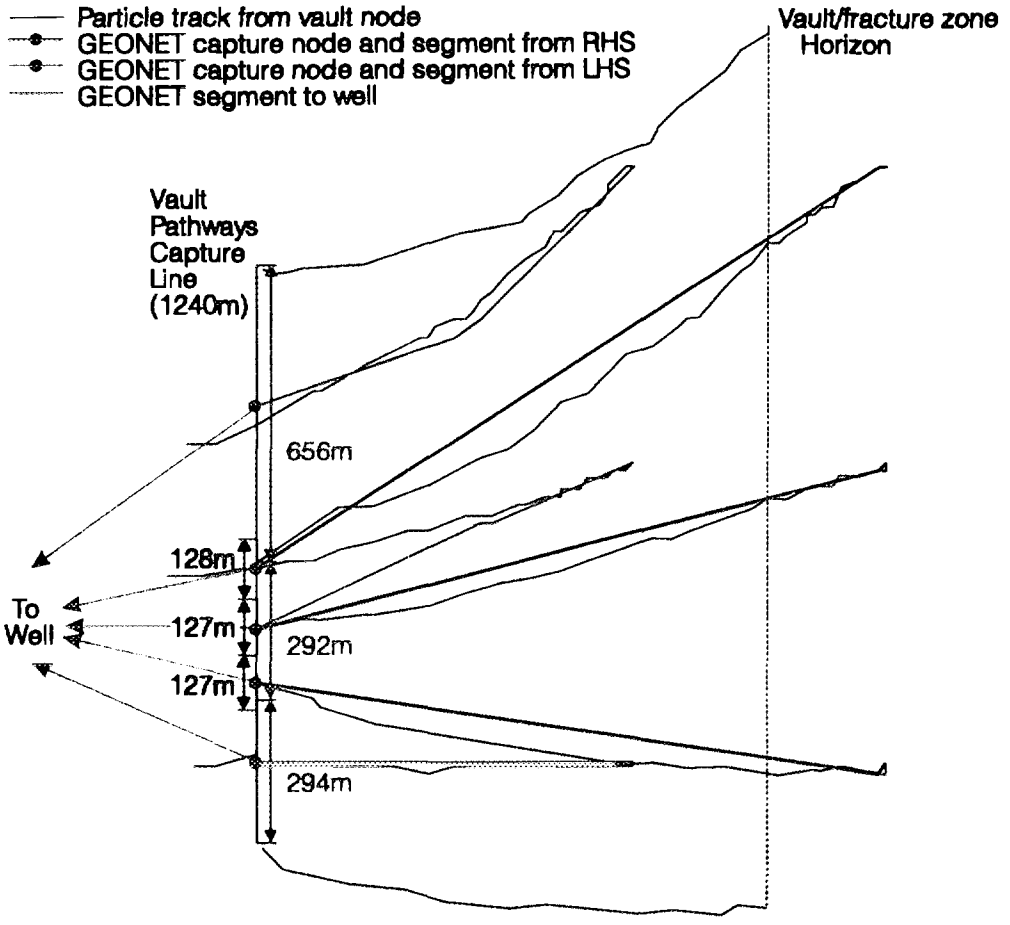

FIGURE 18: Partitioning of Pathways into Well Capture Nodes

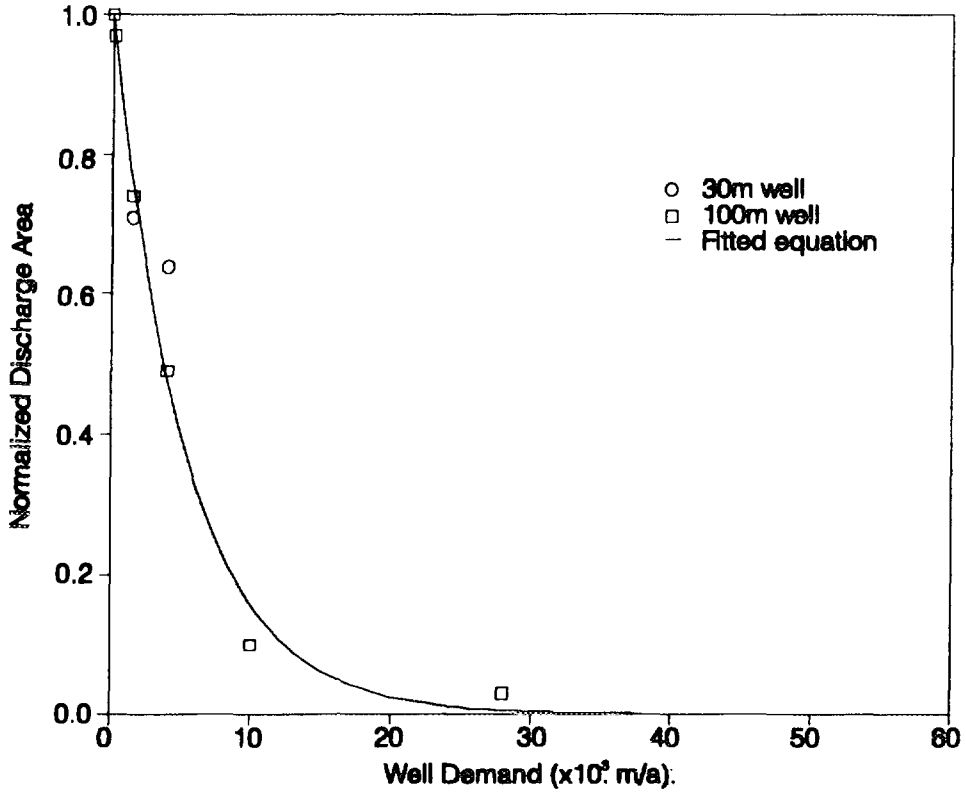

FIGURE 19: Size of the Area of Emergence of Vault Pathways at the Boggy Creek South Discharge Area as a Function of Well Depth and Demand

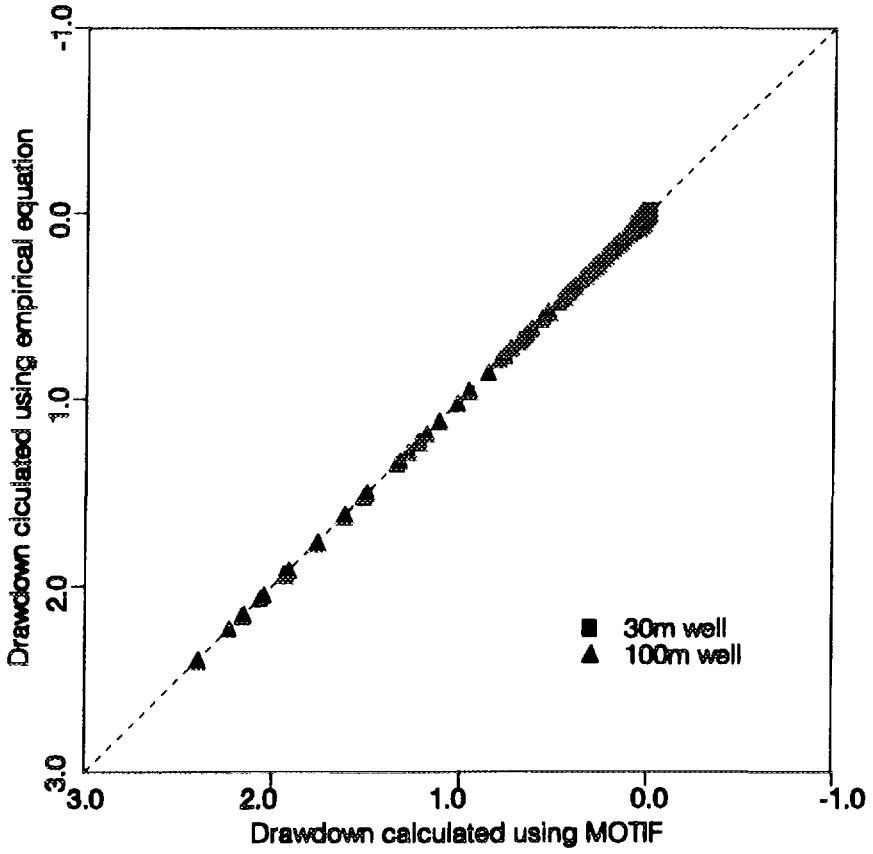

FIGURE 20: The Drawdowns at the Nodes Influenced by Well the Empirical Equation Versus the Drawdowns Obtained from MOTIF Simulations

Cat. No. / N° de cat.: CC2-11494/3E
ISBN 0-660-16502-3
ISSN 0067-0367

To identify individual documents in the series, we have assigned an AECL- number to each. Please refer to the AECL- number when requesting additional copies of this document from

Scientific Document Distribution Office (SDDO)
AECL
Chalk River, Ontario
Canada K0J 1J0

Fax: (613) 584-1745 Tel.: (613) 584-3311
ext. 4623

Price: B

Pour identifier les rapports individuels faisant partie de cette série, nous avons affecté un numéro AECL- à chacun d'eux. Veuillez indiquer le numéro AECL- lorsque vous demandez d'autres exemplaires de ce rapport au

Service de Distribution des documents officiels (SDDO)
EACL
Chalk River (Ontario)
Canada K0J 1J0

Fax: (613) 584-1745 Tél.: (613) 584-3311
poste 4623

Prix: B